INVERSION-BASED ITERATIVE FEEDFORWARD-FEEDBACK CONTROL: APPLICATION TO NANOMECHANICAL MEASUREMENTS AND HIGH-SPEED NANOPOSITIONING

BY YAN ZHANG

A thesis submitted to the

Graduate School—New Brunswick

Rutgers, The State University of New Jersey

in partial fulfillment of the requirements

for the degree of

Master of Science

Graduate Program in Mechanical and Aerospace Engineering

Written under the direction of

Professor Qingze Zou

and approved by

_____

_____

_____

_____

New Brunswick, New Jersey

Oct, 2011

ABSTRACT OF THE THESIS

Inversion-based Iterative Feedforward-Feedback Control: Application to Nanomechanical Measurements and High-speed Nanopositioning

by Yan Zhang

Thesis Director: Professor Qingze Zou

This thesis presents the development of inversion-based iterative feedforward-feedback (II-FF/FB) approach and its application to achieve high-speed force load in nanomechanical property measurement of soft materials in liquid, and high-speed nanopositioning control using piezoelectric actuators. High-speed nanopositioning is needed in various applications. For example, high-speed precision tracking of the force load is needed to measure the rate-dependent viscoelasticity of a wide range of soft materials in liquid, including live cells. In these applications, however, various adverse effects exist that challenge the precision tracking of the desired trajectory. For instance, during the nanomechanical measurement in liquid, the tracking precision is limited by the thermal drift effect, the reduction of the signal to noise ratio, and the hysteresis and the vibrational dynamics effects of the piezoelectric actuators (used to position the probe relative to the sample), particularly during high-speed measurements. These adverse effects limit the positioning precision not only during quasi-static operation (i.e., low-speed), but also in high-speed tracking. This research is focused on the development the II-FF/FB technique to tackle these critical issues in practical applications. Motivated by the challenges in high-speed nanomechanical measurement of soft materials in

liquid, the II-FF/FB is developed by inverting the closed-loop system dynamics, and then updating and correcting the inversion-based input through iterations (called the closed-loop injection II-FF/FB, CIII-FF/FB technique). A proportional-integral (PI) feedback controller along with a notch-filter is utilized to improve the robustness of the entire system against dynamics uncertainties and the gain margin of the closed-loop system. The proposed CIII-FF/FB technique is implemented in experiments to the nanomechanical property measurement of a poly (dimethylsiloxane) (PDMS) sample in liquid. The experimental results show that by using the CIII-FF/FB technique, precision tracking of the desired force load profile can be achieved in high speed nanomechanical measurement of soft materials in liquid. We also study an alternative approach to the II-FF/FB approach by inverting the plant dynamics to generate the feedforward input, and injecting the feedforward input into the feedback loop by augmenting it to the feedback one (called the plant-injection II-FF/FB, PIII-FF/FB technique). These two II-FF/FB techniques, the CIII-FF/FB and PIII-FF/FB techniques, are compared through two experimental implementations: (1) the nanopositioning tracking of a piezo-bimorph actuator, and (2) the force-load profile tracking in nanomechanical measurements in liquid. The experimental results are analyzed and discussed to compare the performance of these two approaches under various conditions.

Acknowledgements

I would like to express my deep and sincere gratitude to my advisor, Dr. Qingze Zou. His novel ideas have leaded me all through this work. He also provided me strong support through constant encouragement and patient guidance. Moreover, his attitude toward research has had a remarkable impact on my entire career. Working with him has made this study enjoyable and meaningful.

I would also like to thank my committee members for their efforts and contributions to this work: Prof. Jingang Yi, Prof. Haim Baruh and Prof. Haym Benaroya.

At the same time I am deeply grateful to my lab colleagues. Without their assistance this work would not have been successful.

I would like to acknowledge NSF CAREER award CMMI-1066055 awarded to Prof. Zou for the financial support for my study and work.

Finally, I would like to present my special gratitude to my dear parents and friends. Their loving support makes me feel strong, independent and confident.

Dedication

To my parents, I really appreciate their support.

Table of Contents

List of Tables

List of Figures

Chapter 1

Introduction

1.1 Motivation & Objectives

The development of inversion-based iterative feedforward-feedback (II-FF/FB) approach is presented in this thesis with applications to high-speed force load in nanomechanical property measurement of soft materials in liquid, and high-speed nanopositioning control with piezoelectric actuators. High-speed nanopositioning is widely applied in various procedures. For instance, the measurement of the rate-dependent viscoelasticity of a wide range of soft materials in liquid, including live cell, is achieved with the assistance of high-speed precision tracking of the force load. However, the precision tracking of the desired trajectory is challenged by various adverse effects. Thermal drift effect, the reduction of the signal to noise ratio, and the hysteresis and the vibrational dynamics effects of the piezoelectric actuators (used to position the probe relative to the sample), particularly during high-speed measurements are typical adverse effects in the nanomechanical measurement in liquid. The positioning precision is badly reduced due to the mentioned above undesired effects, not only in quasi-static operation (i.e., low-speed), but also in high-speed tracking.

Control techniques need to be developed to achieve high-speed nanomechanical measurement in liquid. Open-loop control is limited to the measurements at low-speed. Recently iterative learning control (ILC) can be applied to increase the measurement rate and can also compensate the hysteresis and vibrational dynamics. However, ILC is limited by the non-periodic thermal drift casued by the heating of the laser spot deflected around the cantilever probe. In order to compensate the thermal drift in liquid, the feedback can be applied to the measurement without considering the loss of the bandwidth. Finally, we combine the inversion-based feedforward-feedback control approach

with the iteration control framework to address the challenges of nanomechanical measurements in liquid. The II-FF/FB approach is implemented to the nanomechanical measurement of a poly (dimethylsiloxane) (PDMS) sample in liquid using SPM. After that two different schemes of II-FF/FB are presented and compared. Two schemes are implemented to the trajectory of a piezoactuator stripe.

1.2 Thesis outline

In Chapter 2, high-speed force load in nanomechanical property measurement in liquid is implemented using iterative feedforward-feedback control. First, a brief background is presented on high-speed force load in nanomechanical measurement which includes the measurement using scanning probe microscopy (SPM), the control challenges and the proposed control method. Then, the proposed method is applied to compensate for the drift during the force-curve measurement of a PDMS sample in liquid. Also the force tracking results at different rates are compared. Chapter 3 goes into the details about inversion-based iterative feedforward-feedback control. We describe the closed-loop injection approach and the plant injection approach. After that the two approaches are illustrated by tracking triangular trajectories on the piezoelectric actuator and by tracking the force-load profile in nanomechanical measurements in liquid. Chapter 4 provides a conclusion. Appendix includes Matlab codes and a Simulink diagram to finish the experiment and the analysis.

Chapter 2

High-speed Force Load in Nanomechanical Property Measurement in Liquid using Iterative Feedforward-feedback Control

2.1 Introduction

We present in this chapter an inversion-based iterative feedforward-feedback (II-FF/FB) approach to achieve high-speed force load during nanomechanical property measurement of soft materials in liquid. The nanomechanical properties of a wide range of soft materials, particularly live biological samples such as live cells, need to be measured and studied in liquid [1, 2]. Particularly, measurement of nanomechanical properties at high-speed is needed when dynamic evolution of the sample occurs during the measurement [3], and/or measuring the rate-dependent viscoelasticity of materials [4]. Compared to the measurement in air, however, nanomechanical measurement in liquid is much more challenging, due to the adverse effects including the thermal drift effect [5, 6, 7], the reduction of the signal to noise ratio, and the hysteresis and the vibrational dynamics effects of the piezoelectric actuators (used to position the probe relative to the sample), particularly during high-speed measurements [8]. Thus, we propose to address these challenges in nanomechanical property measurements in liquid through an II-FF/FB approach. The proposed method is illustrated through experimental implementation to the force-curve measurement of a poly (dimethylsiloxane) (PDMS) sample in liquid.

Challenges exist in achieving high-speed nanomechanical measurements of soft materials in liquid [9]. We note that the nanomechanical properties of a wide variety of soft materials need to be measured in liquid. For example, the nanomechanical properties of the live cell shall be measured in a physiologically-friendly liquid environment [10]. Nanomechanical measurement in liquid is also needed to avoid the capillary force

due to the thin water layer between the probe and the sample that exists during the nanomechanical measurement in air, particularly when the sample is hydrophilic [11]. The accuracy of nanomechanical measurement in liquid, however, can be severely limited by the thermal drift of the cantilever deflection signal during the measurement. Compensation for the drift of the cantilever deflection in liquid is complicated by the reduction of the signal-to-noise ratio due to the loss of laser density to the liquid environment, and larger disturbances and vibrations due to the hydrodynamic forces from the liquid environment. Further challenges also come from the nonlinear hysteresis and vibrational dynamics of the piezoelectric actuators when the nanomechanical properties are measured at high speed and large displacement range [12]. These challenges hinder the accuracy and measurement spectrum of nanomechanical property measurements in liquid.

Control techniques need to be developed to achieve high-speed nanomechanical measurement in liquids. Currently the nanomechanical properties are often acquired through the force-distance curve measurement [9] by simply scaling the desired force profile with the DC-gain of the system. With no compensation for the adverse effects described above, such an open-loop method is limited to the measurements at low-speed and in air. The measurement rate of force-curve measurements in air can be substantially increased by using control techniques such as the iterative learning control (ILC) technique as demonstrated in [12], where the hysteresis and vibrational dynamics of piezo-actuator can be effectively compensated for in the iteration framework [13]. The ILC approach, however, cannot be directly applied to the nanomechanical measurement in liquid, due to the significant thermal drift and liquid-related disturbance forces that are non-periodic in nature. Although these non-periodic adverse effects can be compensated for via feedback control, the use of integral control (as needed to address the slowly-varying thermal drift effect) renders the bandwidth of the closed-loop system significantly smaller than the open-loop instrument dynamics (e.g., the SPM dynamics in the vertical direction). As a result, such a feedback control scheme is still limited to the low-speed force curve measurements in liquid. To the best knowledge of the author, little work to high-speed nanomechanical measurements in liquid has been reported.

We combine the inversion-based feedforward-feedback control approach with the iteration control framework to address the challenges of high-speed nanomechanical measurements in liquid. First, a proportional-integral (PI) feedback controller is utilized to compensate for the thermal drift and other non-periodic disturbances effects. A notch-filter is designed to enlarge the low gain-margin of piezo-actuators due to piezo-actuator's lightly-damped resonant dynamics. Secondly, to fully exploit the a priori knowledge of the system and the operation (i.e., the known desired force profile), a feedforward controller based on the inverse system dynamics is augmented as a pre-filter to the closed-loop. To further combat the uncertainty and unknown dynamics that are difficult to capture by a fixed dynamics model, the inverse-based pre-filter is adaptively updated by using the measured input-output data through an iteration process. The proposed II-FF/FB approach is implemented to the nanomechanical measurement of a PDMS sample in liquid using SPM. The experimental results obtained by using the proposed II-FF/FB scheme is presented and discussed.

2.2 High-speed force load in nanomechanical measurement in liquid

In this section, we present the proposed II-FF/FB approach to high-speed force load in nanomechanical property measurement in a liquid. We start by briefly describing the force-distance curve measurement using SPM.

2.2.1 Nanomechanical property measurement using SPM

The indentation-based approach to measure the nanomechanical properties of materials has been established as an indispensable tool in various fields, i.e., the nanomechanical properties can be interrogated by measuring the force applied (from the probe) to the sample along with the displacement of the probe relative to the sample, i.e., the force-distance curve measurement [9]. For example, when using SPM to measure the force-distance curve, the SPM-probe is driven under a piezoelectric actuator to push upon the sample surface until the deflection of the cantilever (i.e., the force applied onto the sample surface) reaches the desired value, then the SPM-probe will be retraced to a

given distance. The probe can be either in continuous or intermittent contact with the sample surface during the push-retrace process (see Fig. 2.1(a), where the probe-sample force is measured from the probe deflection via an optics sensing scheme). Various material properties can then be obtained from the measured force/indentation data through a chosen contact mechanics model of the probe-sample interaction [9]. Compared to other existing techniques for nanomechanical property measurement in liquid (particularly for live biological sample) [14, 15, 16] , the indentation-based approach provides the unique capability to apply the stimuli force and then, quantitatively measure the material response at the desired location. Piconewton force resolution and nanometer spatial resolution can be achieved when SPM is used. Such a high force/spatial resolution are particularly desirable when measuring the nanomechanical properties of soft inhomogeneous materials in liquid (such as live cell).

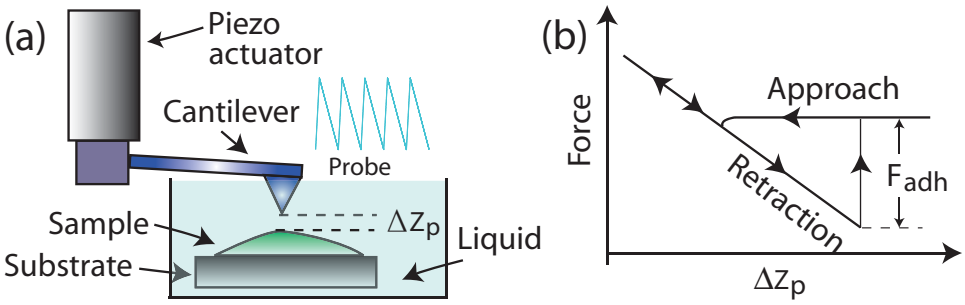

Figure 2.1: The scheme of force curve measurement using AFM.

2.2.2 Control challenges in high-speed nanomechanical measurement in liquid

Precision measurement of nanomechanical properties in liquid is complicated by the adverse effects existing in the operation environment and the actuation-positioning system. Specifically, the nanomechanical measurement is compounded by the thermal drift effect on the force applied and the indentation measured [5, 6]. When the laser beam is deflected on the cantilever probe, the thermal drift is generally caused by the temperature variations due to the heat of the local liquid around the cantilever. Such drift becomes significant during relatively long measurement time period [5]. When the

nanomechanical measurement is conducted in liquid environment using SPM, the temperature variation is mainly caused by the the heating of the liquid locally around the cantilever-probe, which in turn causes the cantilever vibration [7]. The thermal drift effect can also be induced by the evaporation and the capillary rise/fall of the liquid up/down the indenter shank [6]. Moreover, the nanomechanical property measurement under liquid is also severely effected by the disturbance on the probe motion due to the distributive hydro dynamics force [17], particularly when the force load rate is high. The other main limit to the force load rate is due to the excitation of the instrument dynamics (i.e., compliance) during high-speed motion, which results in the convolution of the force applied and the indentation measured with the instrument hardware dynamics [18]. Further adverse effect also arises from the nonlinear hysteresis effect of the piezoelectric actuators commonly used to drive the probe in indentation-based nanomechanical measurements [8, 19]. Therefore, these adverse effects need to be compensated for to achieve high-speed nanomechanical measurements in liquid.

As an example, Figure 2.2 presents the cantilever deflection signal measured when the cantilever was in contact with a silicon sample in water under a constant force load (under room temperature). Clearly, the cantilever deflection substantially varied over 100% than its set-point value during the 5 seconds of measurement time. Such a large variation of deflection was even larger than that during the usual force-distance measurement.

2.2.3 Inversion-based iterative feedforward-feedback control

We combine the inversion-based feedforward-feedback control approach with the iteration control framework to address the challenges of high-speed nanomechanical measurements in liquid (see Fig. 2.3). First, we propose the use of proportional-integral (PI) control along with a notch filter to compensate for the drift effect. As piezoelectric actuators tend to have a low gain margin (due to the lightly-damped resonant peaks that dominate the piezo-actuator dynamics) [8], a notch filter $G_N(s)$ is designed to increase the gain margin of the SPM dynamics in the vertical z-axis dynamics of piezoelectric

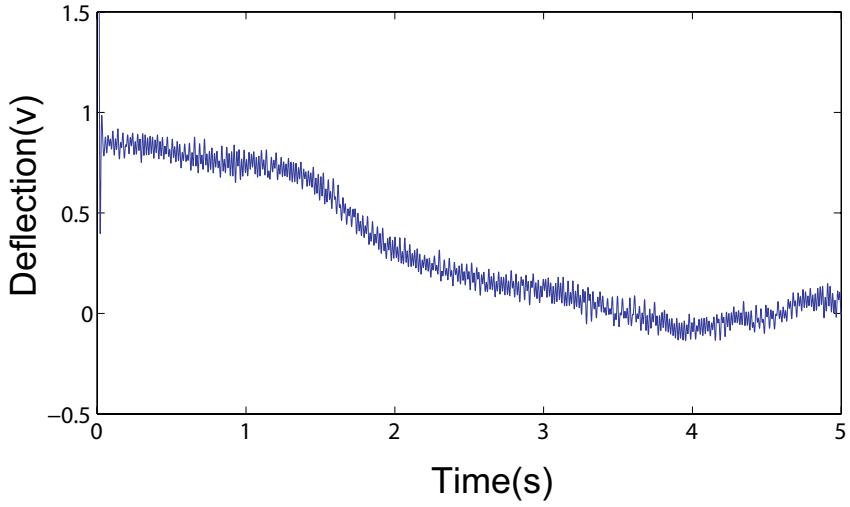

Figure 2.2: The variation of the cantilever by thermal noise

actuator of SPM $G_z(s)$,

$$G_N(s) = k\frac{(s - 2\pi z_1) \times (s - 2\pi z_2)}{(s - 2\pi p_1) \times (s - 2\pi p_2)} \tag{2.1}$$

where the pair of poles and zeros, $\{p_1, p_2\}$, and $\{z_1, z_2\}$, are chosen to cancel the dominant resonant peaks of the SPM dynamics, and the static gain k is chosen to render the DC-Gain of the filter to be one. Then, a PI controller is applied to the concatenated system, $G_N(s)G_c(s)$,

$$G_c(s) = K_P + \frac{K_I}{s} \tag{2.2}$$

where K_P and K_I are the proportional and integral gain, respectively. By using the above notch filter $G_N(s)$, the gain-margin of the concatenated system, $G_N(s)G_z(s)$, can be substantially increased. Therefore, a much larger PI gain K_p and K_I can be used to reduce the drift-caused cantilever vibration in the relatively low frequency region, and furthermore, improve the bandwidth of the closed-loop system.

Next, we propose to utilize an II-FF/FB approach to achieve high-speed nanomechanical measurements in liquid. We note that although the above PI-notch-filter feedback

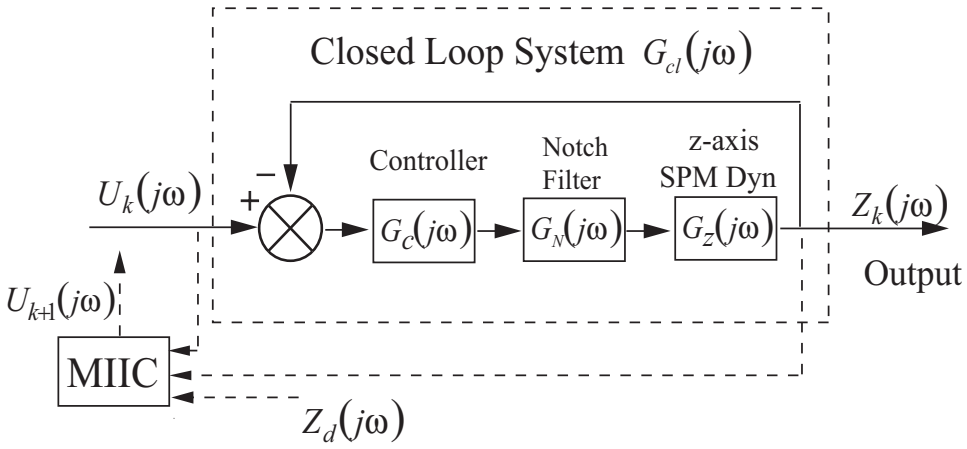

Figure 2.3: Block diagram of the II-FF/FB scheme.

control can adequately compensate for the drift effect, the bandwidth of the closed-loop system also becomes limited. The reduction of the bandwidth is due to the need of integral-type of controller in the feedback loop to combat the drift effect at low frequencies, which, in turn, limits the range of the force load rate that can be accurately tracked during the force-curve measurement. As the desired force trajectory is known a priori, the inversion-based feedforward-feedback approach becomes an efficient solution to exploit the knowledge of the system dynamics and the operation for tracking desired force profile at high-speed.

2.3 Experiment implementation

We illustrate the proposed approach to high-speed force load in nanomechanical measurements in liquid through the force-distance measurement of a poly (dimethylsiloxane) (PDMS) sample. The objective is to demonstrate that by using the proposed approach, the desired force load rate can be accurately tracked in liquid at high-speed. We present the experimental implementations in two parts: 1) The compensation for the thermal drift effect; And 2) the force-curve measurement in liquid by using the II-FF/FB method. We start by briefly describing the SPM system employed in the experiments.

2.3.1 Experiment setup

The experiments were carried out under room temperature on a SPM system (Dimension 3100, Veeco Instruments Inc.) with a V-shape silicon nitride cantilever probe. The nominal stiffness and nominal curvature radius of the cantilever were at 0.06 N/m and 20 nm, respectively. The effective spring constant measured by using the thermal noise method was at 0.08 N/m. A set of images of a calibration sample were acquired a priori to the experiments so that the variation of the probe shape was minimized and can be ignored. All the control inputs were generated by MATLAB xPC-target and sent through a data acquisition card (DAQ, sampling rate: 10 KHz) to directly drive the high-voltage amplifier of the AFM-controller.

2.3.2 Drift Compensation: Results and Discussion

The design of the notch-filter-PI feedback control to combat the drift and other non-periodic disturbance effects started with the measurement of the frequency-response of the z-axis SPM dynamics in liquid. The SPM cantilever was driven to contact a silicon sample in liquid to ensure a stable probe-sample contact (the static normal force load: 14 nN). Then the frequency response was obtained by using a Dynamic Signal Analyzer (DSA, HP 35665A , see [13] for details). To evaluate the dynamics variations, the frequency responses were measured several times under different input amplitudes, as shown in Fig. 2.4 for four different input levels (40 mv, 60 mv, 80 mv and 100 mv). Clearly, large variations were pronounced in the low frequency region, which directly resulted in the significant drift effect shown in Fig. 2.2. Figure 2.4 also shows that the resonant peak around 791.7 Hz dominated the z-axis SPM dynamics response in the high frequency region. Thus, the following notch filter was implemented accordingly,

$$G_N(s) = 1.6 \times \frac{(s - 2\pi \times (-6.26 + j791))(s - 2\pi \times (-6.26 - j791))}{(s - 2\pi \times (-200))(s - 2\pi \times (-5000))} \tag{2.3}$$

By using the above notch-filter, the gain margin was increased by 15 dB. Next, the following PI controller was designed accordingly,

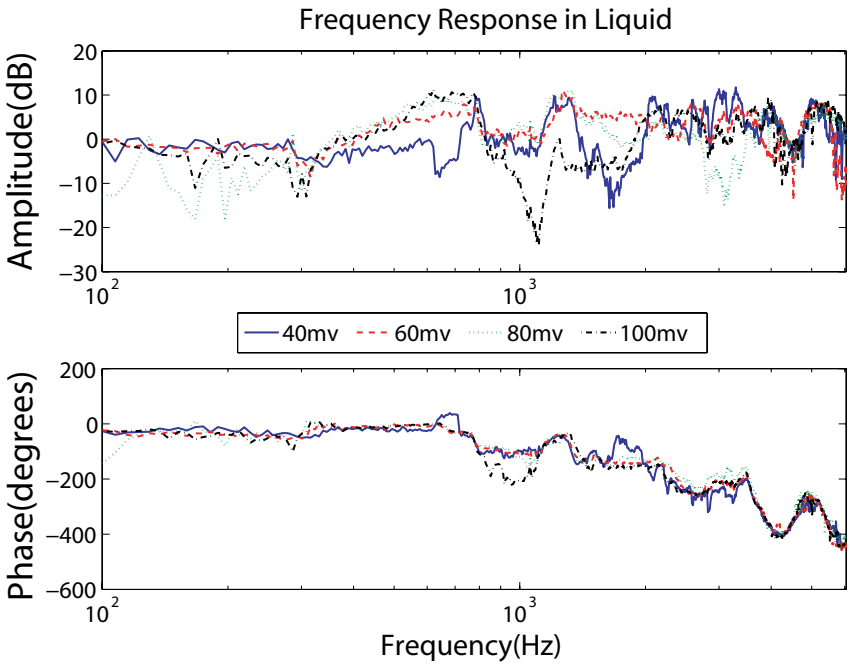

Figure 2.4: The frequency response of the z-axis SPM dynamics in liquid measured under four different input levels.

$$G_c(s) = 2 + \frac{10}{s}, \tag{2.4}$$

where the gain of the PI controller were experimentally tuned.

The PI-notch-filter feedback control system was applied to compensate for the drift effect during the force-curve measurement of a PDMS sample in liquid (Readers are referred to [12] for details of the PDMS sample preparation). The desired force trajectory was chosen to consist of a push-in section and a retraction section with different slopes and a flat section in between. The tracking of the desired force trajectory by using the designed PI-notch-filter is compared to that with no drift compensation in Fig. 2.6 for the force load rate of 1 Hz. The relative drift-caused tracking error (i.e., the ratio of the tracking error to the desired force profile) was reduced from 37.29% in $E_M(\%)$ and 30.34% in $E_{RMS}(\%)$ to 8.67% and 9.06%, respectively, where the relative maximum tracking error $E_M(\%)$, and the relative RMS tracking error $E_{RMS}(\%)$ are defined by:

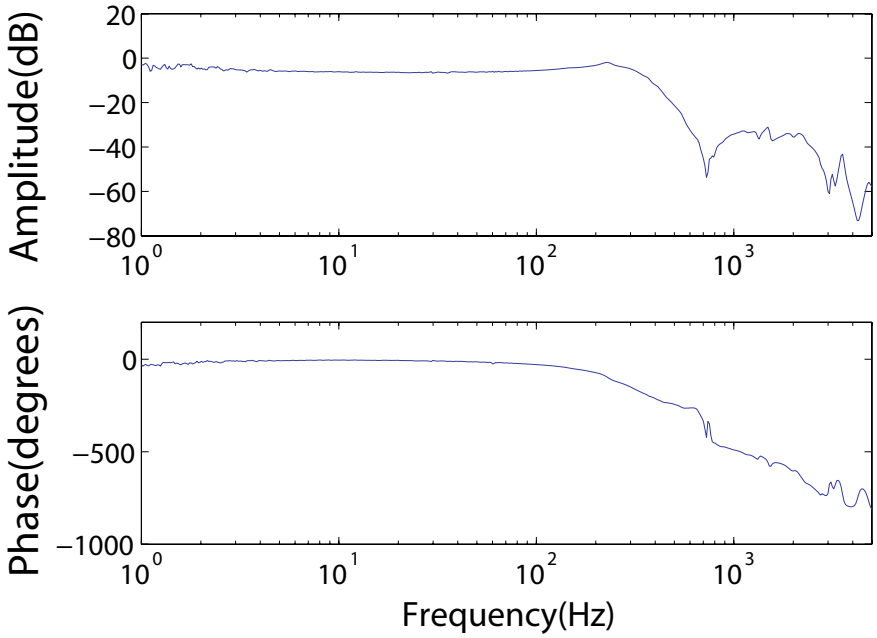

Figure 2.5: Bode plot of the PI-Notch-filter feedback.

$$E_M(\%) \triangleq \frac{\|x_d(\cdot) - x_k(\cdot)\|_\infty}{\|x_d(\cdot)\|_\infty} \times 100\% \ , \qquad E_{RMS}(\%) \triangleq \frac{\|x_d(\cdot) - x_k(\cdot)\|_2}{\|x_d(\cdot)\|_2} \times 100\% \tag{2.5}$$

Therefore, the experimental results clearly demonstrated that the drift effect can be substantially reduced by using the PI-notch-filter feedback controller.

2.3.3 Desired Force Load Tracking: Results and Discussion

Next, the proposed II-FF/FB was implemented to the force-curve measurements to track the desired force-distance curve on a PDMS sample at 5 different force load rates (1 Hz, 10 Hz, 30 Hz, 60 Hz and 120 Hz). The force tracking results are compared with respect to the desired force profile along with the tracking by using the PI-notch-filter feedback control alone in Fig. 2.7 to Fig. 2.11 for these five load rates, respectively. The tracking performance of these two methods is also compared in Table 2.1 (the $E_M(\%)$ and the $E_{RMS}(\%)$ errors), where the corresponding force load velocities (for the five load rates) are also listed. All the force tracking results presented were measured one

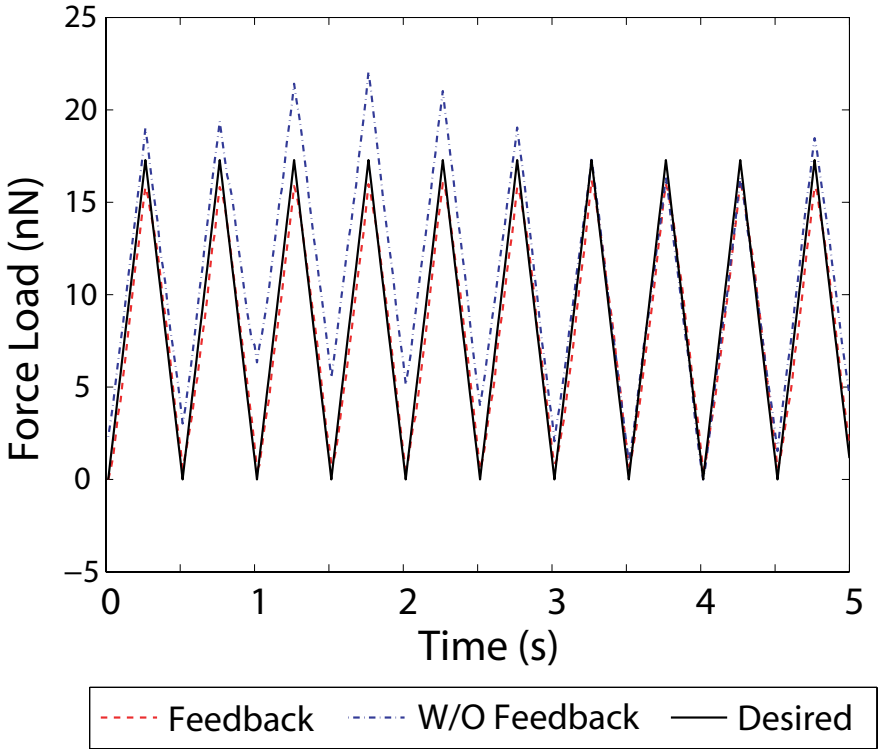

Figure 2.6: Comparison of the tracking of a triangle desired force profile by using the PI-notch-filter-feedback control to that obtained with no drift compensation.

after the other under the same probe-sample contact condition (i.e., before applying the control method to track the desired force-curves, a stable probe-sample contact had been established by using the PI-notch-filter feedback to maintain the deflection signal around the set point value of 14 nN). The iteration was stopped when both the relative maximum tracking error $E_M(\%)$, and the relative RMS tracking error $E_{RMS}(\%)$ stopped decreasing further.

The experimental results demonstrate that precision tracking of the desired force load profile can be achieved by using the proposed II-FF/FB control approach in high speed nanomechanical measurement of soft materials in liquid. When the force load rate was low (1 Hz), the desired force load can be tracked reasonably well by using the PI-notch-filter feedback control alone (Fig. 2.7) with relatively small tracking error (Table 2.1). However, as the force load rate was increased towards the bandwidth of the closed-loop system at 120 Hz (see Fig. 2.5), high-order harmonic frequencies of

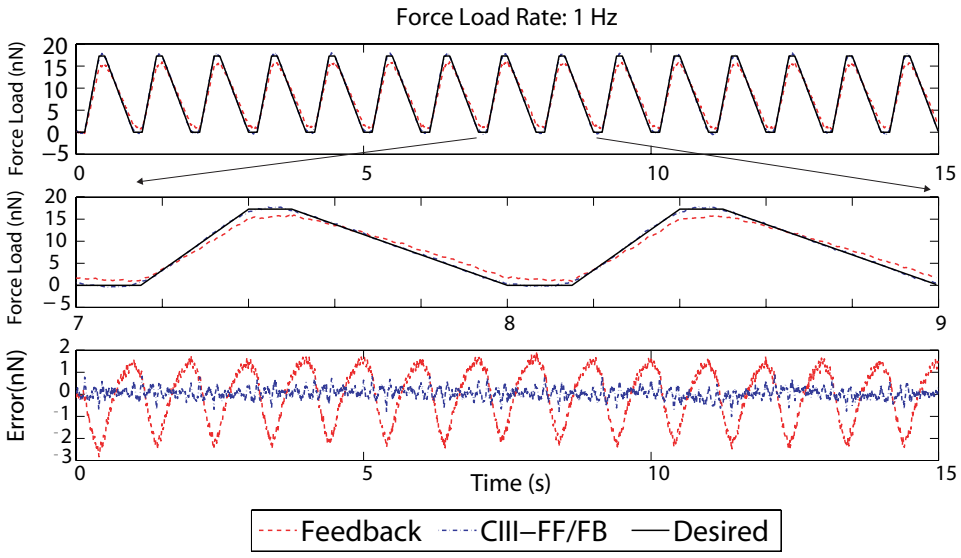

Figure 2.7: The comparison of the force tracking by using the PI-notch-filter feedback only and that by using the CIII-FF/FB control for the force load rate of 1 Hz.

Table 2.1: Comparison of the tracking errors ($E_M(\%)$ and $E_{RMS}(\%)$) by using the PI-notch-filter feedback control, and the CIII-FF/FB approach at different force load rates.

		$E_M(\%)$		$E_{RMS}(\%)$	
Load Rate (Hz)	Load Velocity (μm/sec)	PI	CIII	PI	CIII
1	0.86	17.54	6.25	12.14	2.35
10	8.64	29.74	5.67	15.99	2.42
30	24	49.1	6.88	28.3	3.06
60	64.8		10.64	—	4.23
120	128		8.11	—	4.03

the desired force trajectory outside the bandwidth became significant. As a result, the tracking error of using the PI-Notch-filter feedback control alone increased substantially, and large oscillations occurred (i.e., large vibrations of the probe on the sample surface), as shown in Fig. 2.8. Such large vibrations of the probe on the sample became even more pronounced when the force load rate was further increased and beyond the closed-loop bandwidth. At the load rate of 30 Hz, the vibration amplitude was almost an half of the desired force amplitude. Large tracking error occurred when using the feedback control alone. On the contrary, precision tracking of the desired force profile was achieved by using the proposed II-FF/FB approach. As shown in Fig. 2.7 to Fig. 2.11, both the

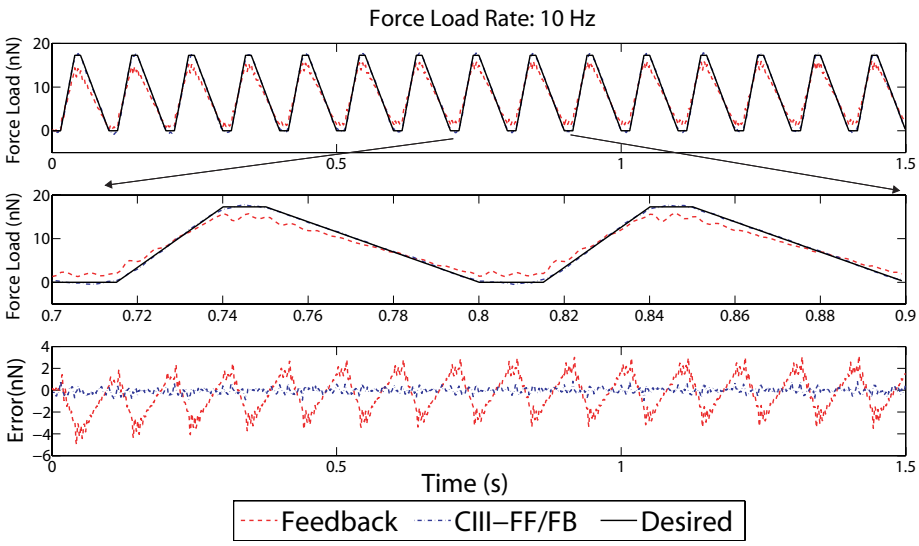

Figure 2.8: The comparison of the force tracking by using the PI-notch-filter feedback only and that by using the CIII-FF/FB control for the force load rate of 10 Hz.

2-norm and the infinity-norm relative tracking errors were maintained around 5% when using the proposed II-FF/FB control approach as the load rate was increased from 1 Hz to 30 Hz. Even when the scan rate was increased much higher to 120 Hz, the tracking error of using the proposed approach was still maintained small. Such a broad range of force load rates (over two orders) is particularly useful to study the rate-dependent viscoelasticity of soft materials in liquid, for example, the nanomechanical properties of live cell [20]. Thus, the experimental results demonstrated that the proposed II-FF/FB approach can effectively account for both the drift and the vibrational dynamics effects, and thereby, achieve high-speed force load during nanomechanical measurement in liquid.

2.4 Summary

An inversion-based iterative feedforward-feedback approach to achieve high-speed force load in nanomechanical measurements in liquid is proposed. The approach combined the inversion-based iterative control with the PI-notch-filter feedback control. The notch-filter-PI feedback controller effectively compensated for the drift and other non-periodic adverse effects on the nanomechanical measurements in liquid, and improved

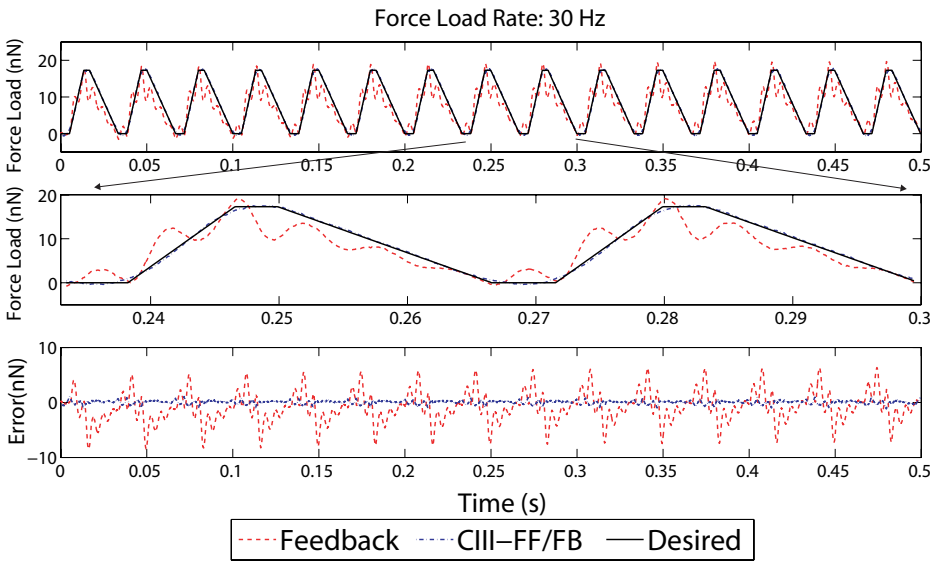

Figure 2.9: The comparison of the force tracking by using the PI-notch-filter feedback only and that by using the CIII-FF/FB control for the force load rate of 30 Hz.

the robustness of the measurement system against dynamics variations and disturbances. Then, the inversion-based iterative control substantially increased the force load rate of the force-curve measurements. The proposed approach was implemented to the force-curve measurements of a PDMS sample in liquid using SPM. The experiment results demonstrated the efficiency of the proposed integrated approach.

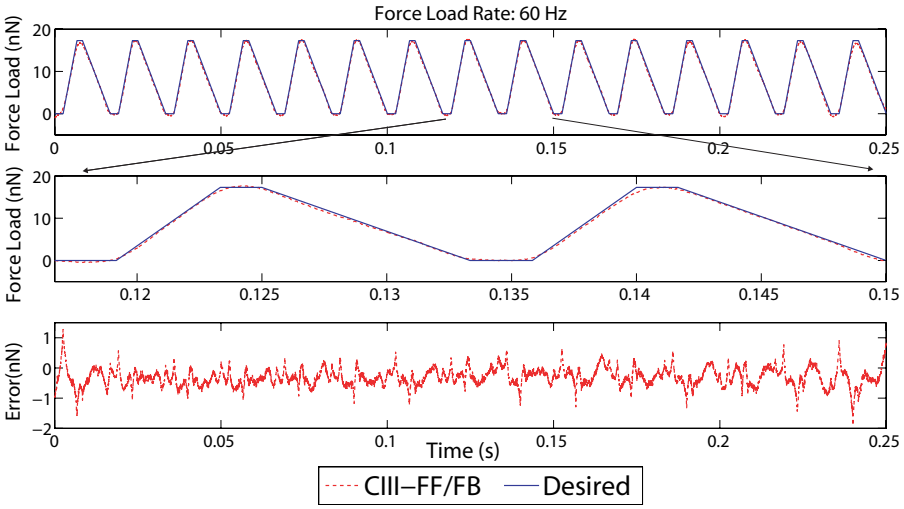

Figure 2.10: The force tracking by using the CIII-FF/FB control for the force load rate of 60 Hz.

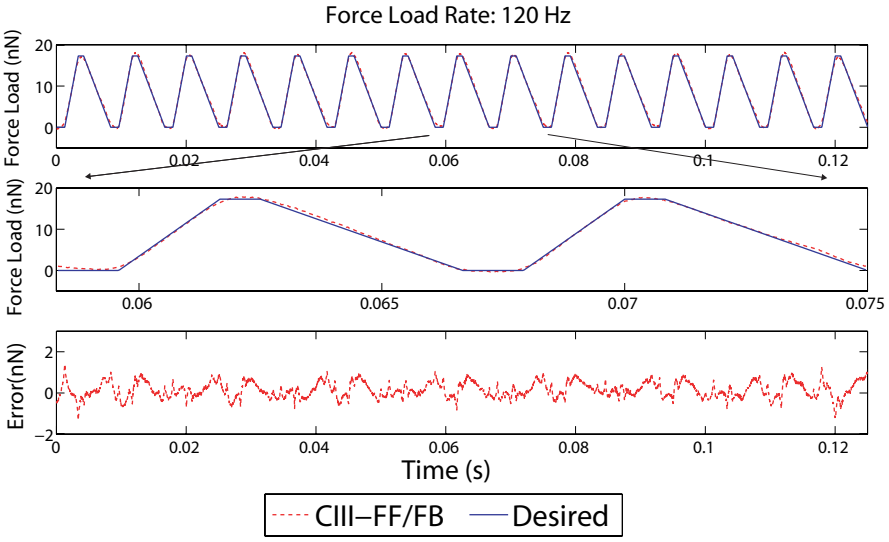

Figure 2.11: The force tracking by using the CIII-FF/FB control for the force load rate of 120 Hz.

Chapter 3

Comparative Study of Two Inversion-based Iterative Feedforward-feedback Control: Bimorph Piezo Actuator Example

3.1 Introduction

In this chapter, we comparatively study two inversion-based iterative feedforward-feedback control architectures through experimental implementations on precision tracking using piezoelectric actuators. In the preceding chapter, we demonstrated the efficacy of the inversion-based iterative feedforward-feedback control approach in both compensating for the large dynamics variations and uncertainties and achieving precision tracking at high-speed. We note that in Chapter 2, the II-FF/FB approach is realized by inverting the closed-loop system dynamics, and then updating and correcting the inversion-based input through iterations (see Fig. 3.1). Alternatively, rather than inverting the closed-loop system dynamics, the feedforward input can be generated by inverting the plant dynamics, and injected into the feedback loop by augmenting the feedforward input to the feedback one (see Fig. 3.2). In this chapter, we comparatively study these two different II-FF/FB control schemes through two experimental implementations: One is the precision trajectory tracking using piezo-bimoprh actuators; the other is the high-speed force load in indentation-based nanomechanical measurement in liquid. In the following, we call the first II-FF/FB scheme (Fig. 3.1) the closed-loop injection II-FF/FB (CIII-FF/FB) method, and the second II-FF/FB scheme (Fig. 3.2) the plant-injection II-FF/FB (PIII-FF/FB) method [21].

The piezoelectric actuator (piezoactuator) has become increasingly important because of its ability for precision positioning (actuation) or sensing in nano and bio-related technologies. For instance, it is used in AFM to image and manipulate samples

at the nanoscale. It is a device made from piezoelectric materials that respond to changing dimensions when voltage is applied. When the materials are stressed, it produces a measurable voltage. With the development of technology, the high-precision high-speed positioning of piezoactuators is required. However, positioning errors existed in an experimental piezo-positioning system due to the adverse effects of creep, hysteresis and vibration. Feedback control, for example proportional-integral-derivative (PID) is standard in manufacturing to reduce the position errors. Modern advanced control technology, such as the inversion-based iterative control (IIC) can be used to improve the positioning errors during high-speed large-range motion.

3.2 Closed-loop injection inversion-based iterative feedforward-feedback control (CIII-FF/FB)

In the CIII-FF/FB approach, the control input to the closed-loop is obtained by inverting the entire closed-loop dynamics (e.g., transfer function),

$$u_{ff}(j\omega) = G_{cl}^{-1}(j\omega)Z_d(j\omega) \tag{3.1}$$

where $G_{cl}(j\omega)$ is the closed-loop transfer function,

$$G_{cl}(j\omega) = \frac{G_c(j\omega)G_N(j\omega)G_z(j\omega)}{1 + G_c(j\omega)G_N(j\omega)G_z(j\omega)} \tag{3.2}$$

As discussed in [8], in the presence of drift and other adverse effects on the measurement in liquid, the above closed-loop inverse (instead of the open-loop inverse) is particularly useful, because the robustness of the system can be substantially improved by the feedback controller, i.e., the variations of the SPM dynamics due to the adverse effects are substantially reduced via the feedback. Note that as the desired force profile is known a priori, the limit posed by the nonminimum-phase zeros can be avoided by implementing the controller Eq. 3.1 in frequency-domain offline.

The performance of the above inversion-based feedforward-feedback control approach, however, can still be sensitive to, and thereby limited by the modeling error of the

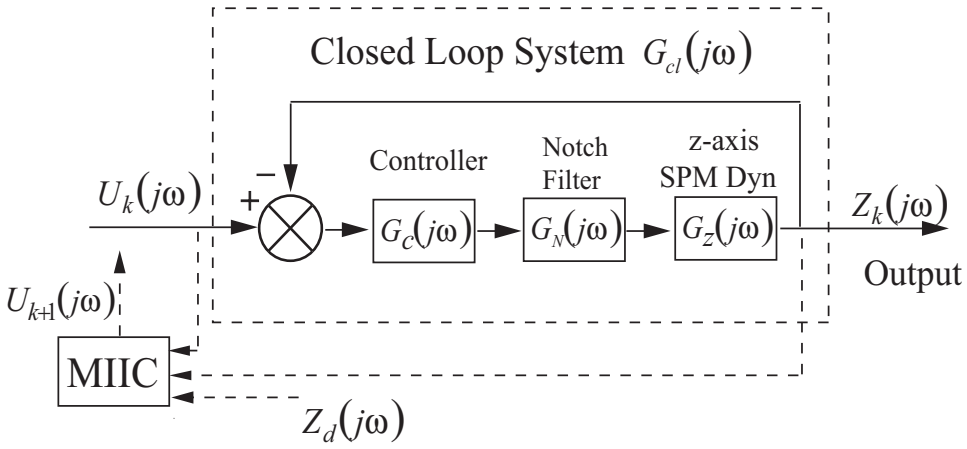

Figure 3.1: Block diagram of the CIII-FF/FB scheme.

closed-loop system $G_{cl}(j\omega)$ [22]. Such modeling error arises due to various effects, including the uncertainties and variations of the system dynamics itself, the measurement error during the modeling process (due to the noise and other disturbance effect during the modeling process), and the fitting of the measured frequency response into a relatively low-order transfer function model. Thus, next we adaptively correct the model dynamics by using the measured input and output data through an iteration process. Specifically, the control input (to the closed-loop system) is given in the frequency-domain by (see Fig. 3.1)

$$u_{k+1}(j\omega) = \frac{u_k(j\omega)}{z_k(j\omega)} z_d(j\omega) \tag{3.3}$$

for $k = 1, 2, \cdots$, and $u_0(\cdot) = k_{dc} z_d(\cdot)$ initially, where k_{dc} the DC-gain of the closed-loop SPM dynamics.

The implementation of the above control scheme (3.3) therefore involves the Fourier transform of the entire control input and the output measured during the force-curve measurement (i.e., the cantilever deflection signal), and then obtaining the control input via inverse Fourier transform in each iteration. The key concept is to use the input and the measured output data to update the frequency response model of the corresponding system, i.e., $G_{cl}(j\omega)$. Through this updating process, not only is the fitting error (to a low-order model) avoided, but also the changes and variations of the system dynamics

can be easily compensated for —with no loss of tracking performance (For example, the z-axis SPM dynamics can be altered with the replacement of a new SPM probe). Such an automatic recovery of tracking performance against system variation is particularly appealing in practical implementations whereas cannot be easily attained when using non-iterative feedback control methods—as those methods require the system dynamics to be remodeled, not feasible in practices. Otherwise, the tracking performance has to be traded-off with the robustness of the feedback controller [23]. Note that the iterative algorithm in Eq. 3.3 is the same as the modeling-free inversion-based iterative control (MIIC) technique proposed in [24]. The readers are referred to [24] for details of the convergence of the MIIC technique in the presence of additional disturbances/noise.

3.3 Plant injection inversion-based iterative feedforward-feedback control (PIII-FF/FB)

Alternatively, in the second PIII-FF/FB approach, the feedforward control input can also be injected directly to the plant, i.e.,

$$Z(j\omega) = \left[G_c(j\omega)G_N(j\omega)G_z(j\omega) + G_{ff}(j\omega)G_z(j\omega)\right] S(j\omega)Z_d(j\omega) \tag{3.4}$$

where $S(j\omega)$ denotes the sensitivity of the closed-loop system,

$$S(j\omega) = \frac{1}{1 + G_c(j\omega)G_N(j\omega)G_z(j\omega)} \tag{3.5}$$

It is clearly from the above Eq. 3.4 and Eq. 3.5 that by choosing the feedforward controller $G_{ff}(j\omega)$ as Eq. 3.6, the exact output tracking can be achieved (in the absence of model uncertainties and disturbances). Similarly, the feedforward input in the feedforward-feedback scheme Eq. 3.4 is given by (see Fig. 3.2)

$$G_{ff}(j\omega) = G_z(j\omega)^{-1} \tag{3.6}$$

$$u_{k+1}(j\omega) = \frac{u_{k,total}(j\omega)}{z_k(j\omega)} z_d(j\omega) \tag{3.7}$$

We note that depending on the nature of the z-axis dynamics $G_z(j\omega)$ (or the plant dynamics in general), the performance of the CIII-FF/FB and the PIII-FF/FB methods

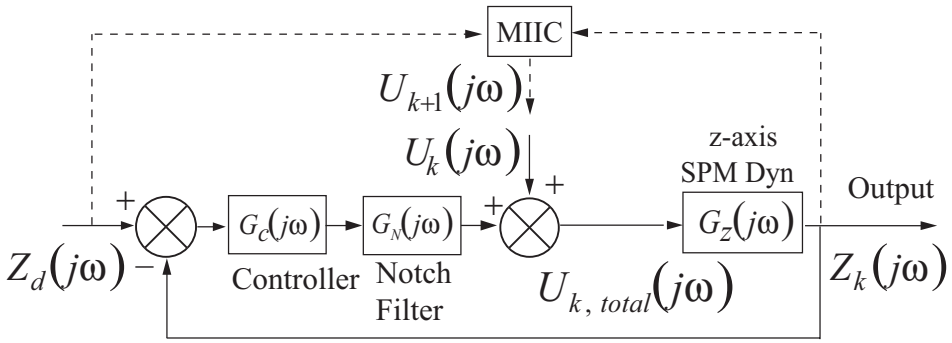

Figure 3.2: Block diagram of the PIII-FF/FB scheme.

can be different. Such a difference exists because that dynamics models that are online "modeled" by using the input-output data in these two methods are different, i.e., the closed-loop dynamics in the CIII-FF/FB method while the z-axis dynamics in the PIII-FF/FB method; and the bandwidth and the robustness of these two different dynamics are different, i.e., the bandwidth of the closed-loop system tends to be smaller than the open-loop z-axis SPM dynamics (particularly when a PI-type of controller is used), while the robustness of the closed-loop system is enhanced over the open-loop one. Thus, when the random variation of the z-axis SPM dynamics and/or the random disturbance is small, better tracking performance can be achieved by using the PIII-FF/FB method, particularly at high-speed. Otherwise, when the random variation or random disturbance is large, such as in liquid, the CIII-FF/FB method can outperform the PIII-FF/FB method.

3.4 Nanopositioning control using bimorph piezoelectric actuator

We illustrate the proposed approach to high-speed displacement measurement using piezoactuators. The objective is to demonstrate that by using the proposed approach, the desired trajectory can be accurately tracked at high-speed. We present the experimental implementations by using two II-FF/FB methods. We start by briefly describing the piezobimorph fixture employed in the experiments.

3.4.1 Experiment setup

A piezobimorph fixture used to carry out the experiment is illustrated in the following Fig. 3.3. Comprised of a bimorph piezoactuator, a low-cost infrared sensor and a high-voltage amplifier (not shown), it is driving the piezoactuator and a PC with a data acquisition card. The stripe piezoactuator is 60 mm long and 20 mm wide and the infrared sensor has a nominal distance of 7.5 mm. All the control inputs were generated by MATLAB xPC-target and sent through the data acquisition card (DAQ, sampling rate: 30 KHz) to directly drive the high-voltage amplifier of the piezoactuators.

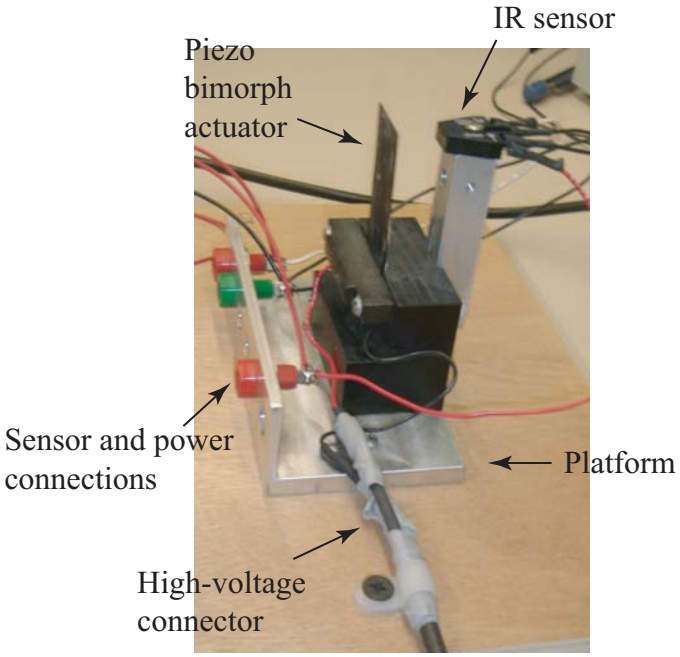

Figure 3.3: The piezobimorph fixture.

3.4.2 Notch filter design and feedback controller design

Feedback control usually can be used to reduce positioning errors in piezoactuators, however, its inability to handle low-gain margin system has posed difficulty for us, as in the experiment the piezoscanner produced a measured gain margin of -21.29 dB [see Fig. 3.4], and thus the highest proportional feedback gain could be set for the stability of the closed-loop system was 0.08. It did not result in significant improvement in the tracking response when compared to the open-loop system. In order to produce

desirable results through feedback control, the gain margin was increased. This was accomplished by modifying the sharp resonant peak of the open-loop system with a notch filter [as shown in Fig. 3.4] [25]. The notch filter was chosen as Eq. 3.8. The frequency response of the composite system shows significant increase in the gain margin from - 21.29 dB to 11.4 dB.

$$G_N(s) = 1.5668 \times \frac{(s - 2\pi \times (-2.29 + j117))(s - 2\pi \times (-2.29 - j117))}{(s - 2\pi \times (-90))(s - 2\pi \times (-240))} \tag{3.8}$$

Then a PI controller was added to the concatenated system as Eq. 3.9. The following

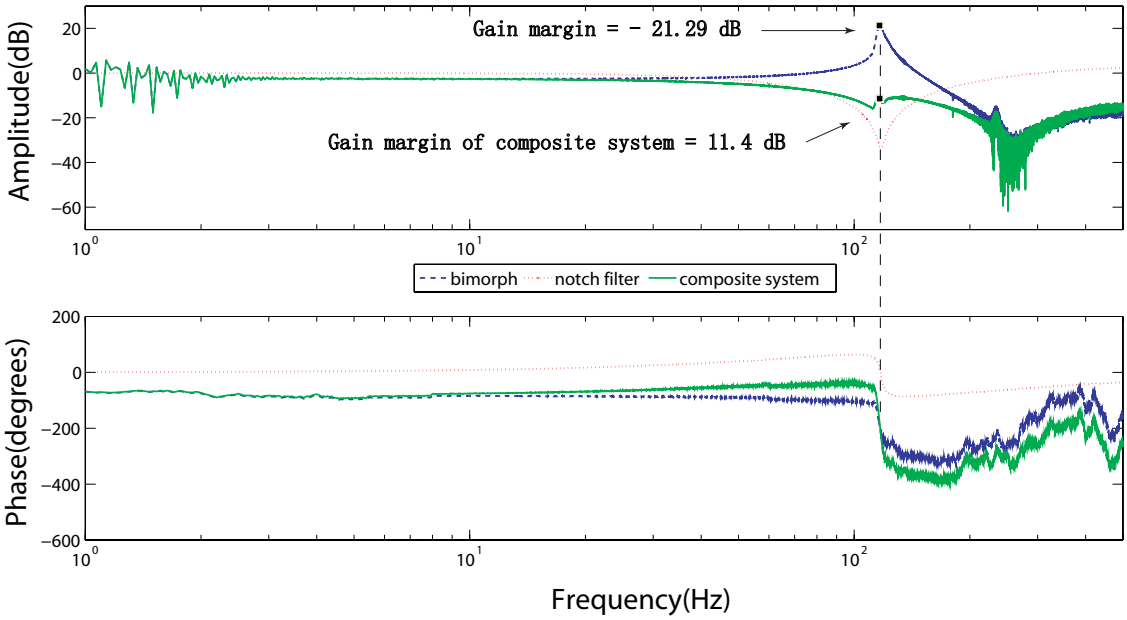

Figure 3.4: Frequency response of the piezo bimorph, the notch filter and the composite system. The measured gain margin of the original system is - 21.29 dB, whereas the gain margin of the composite system is 11.4 dB.

Fig. 3.5 illustrated the comparison of the step response with PI controller and the one uncompensated. The settling time (to 2% error of the final value for a step input) for the output response was reduced from 250 (open-loop case) to 184 ms (closed-loop without notch filter case), and to 25 ms (closed-loop with notch filter case).

$$G_c(s) = 0.5 + \frac{100}{s}, \tag{3.9}$$

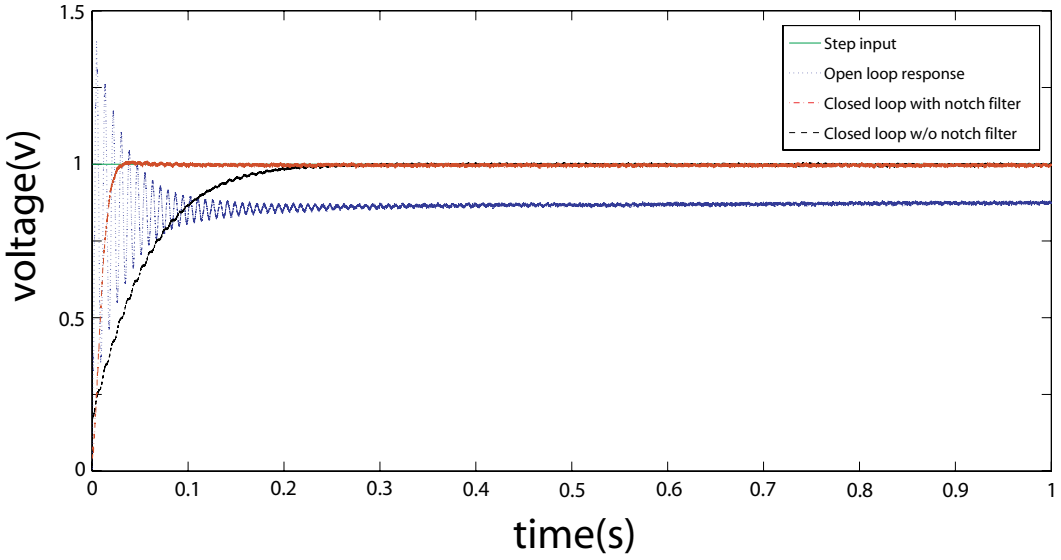

Figure 3.5: Results for the feedback control experiment. The plot compares the step responses of the open-loop and closed loop system.

3.4.3 Tracking results of triangular trajectory

Fig. 3.6 - 3.10 and Table 3.1 demonstrated the results of our experiment, in which the inversion-based iterative approach was integrated with the feedforward-feedback system to track a more general (triangular) trajectory at 5 different scan rates (1 Hz, 20 Hz, 50 Hz, 100 Hz and 120 Hz). The tracking results using two approaches are compared against the desired tracking along with the tracking using PI control. The iteration was stopped when the tracking error stopped decreasing further. The experiments demonstrate that II-FF/FB approach produced better positioning errors reduction for tracking a triangular trajectory than feedback control method.

We note that in bimorph piezoelectric actuator experiments, the tracking performance of the PIII-FF/FB approach was better than that of the CIII-FF/FB approach at each scan rate. As shown in Fig. 3.6, Fig. 3.7 and Table 3.1, the tracking precision of these were similar when the tracking speed was slow at 1 Hz and 20 Hz. When the tracking speed increased, much better tracking precision was achieved by using the PIII-FF/FB approach than by using the CIII-FF/FB appraoch.

Table 3.1: Comparison of the triangular tracking errors ($E_M(\%)$ and $E_{RMS}(\%)$) by using the PI-notch-filter feedback control, CIII-FF/FB approach and the PIII-FF/FB approach at different scan rates on bimorph piezoelectric actuator.

	$E_M(\%)$			$E_{RMS}(\%)$		
Scan Rate (Hz)	PI	CIII	PIII	PI	CIII	PIII
1	3.44	2.38	2.02	3.6	0.66	0.65
20	40.57	3.4	2.68	48.04	0.92	0.89
50	74.18	4.94	4.03	57.11	2.11	1.94
100	89.35	11.7	8.48	54.91	8.67	5.11
120	91.33	69.9	15.4	53.61	49.4	7.95

3.5 Force trajectory tracking: Results and Discussion

Next, the proposed II-FF/FB was implemented to the force-curve measurements. Both the CIII-FF/FB method and the PIII-FF/FB method were applied to track the desired force-distance curve on a PDMS sample at 5 different load rates (1 Hz, 10 Hz, 30 Hz, 60 Hz and 120 Hz). The force tracking results by using these two methods are compared against the desired force profile along with the tracking by using the PI-notch-filter feedback control alone in Fig. 3.11 to Fig. 3.12 for the load rates of 1 Hz, 10 Hz and 30 Hz, respectively. Both $E_M(\%)$ and $E_{RMS}(\%)$ errors of these three methods are compared in Table 3.2. All the force tracking results presented were measured one after the other under the same probe-sample contact condition (i.e., before applying the control method to track the desired force-curves, a stable probe-sample contact had been established by using the PI-notch-filter feedback to maintain the deflection signal around the set point value of 14 nN). When implementing the CIII-FF/FB method and the PIII-FF/FB method, the iteration was stopped when both the relative maximum tracking error $E_M(\%)$, and the relative RMS tracking error $E_{RMS}(\%)$ stopped decreasing further. The results demonstrate that precision tracking of the desired force profile can be achieved by using the proposed II-FF/FB control approach during high speed nanomechanical measurement of soft materials in liquid. As the scan rate increased too much higher and beyond the closed-loop bandwidth, 30 Hz, large tracking error occurred when using the feedback control alone. However, precision tracking was still maintained when using the proposed II-FF/FB approach. Even when

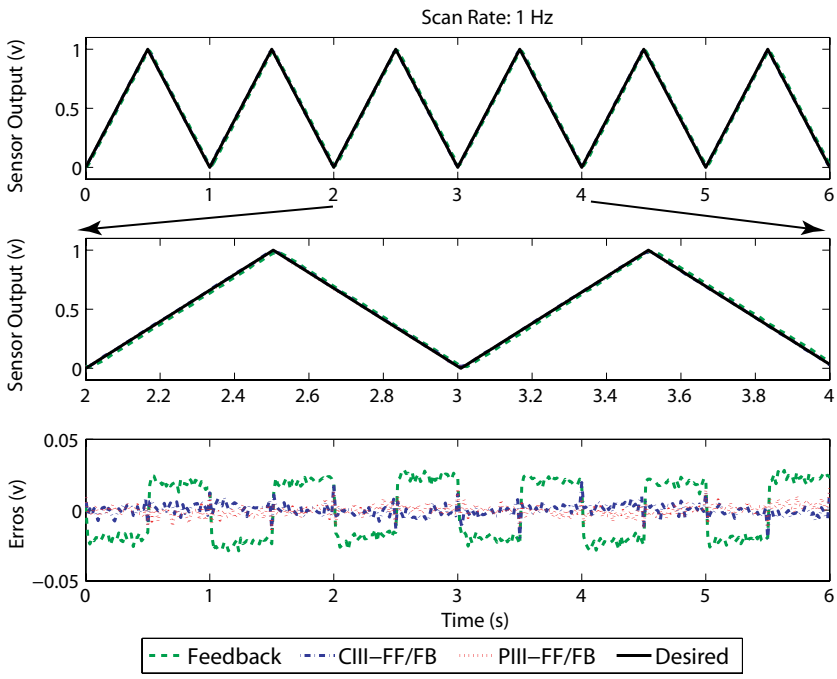

Figure 3.6: The comparison of the force tracking by using the PI-notch-filter feedback only, with that by using the CIII-FF/FB control, and that by the PIII-FF/FB control for the scan rate of 1 Hz.

the scan rate was increased to 120 Hz, the tracking error by using the proposed approach was still maintained to be small. Thus, the experimental results demonstrated that the proposed II-FF/FB approach can effectively account for both the drift and the vibrational dynamics effects during high speed nanomechanical measurement in liquid.

We note that the tracking nanomechanical result is different from the bimorph piezo actuator result at high speed. As the tracking speed increased, better tracking precision was achieved by using the CIII-FF/FB approach than that by using the PIII-FF/FB approach, particularly at the highest speed tested in the experiments at 120 Hz. Such a difference was due to the large non-periodic disturbances and random dynamics variations of the z-axis SPM dynamics that existed in the high frequency region. As a result, these non-periodic and random variations cannot be compensated for iteratively online in the PIII-FF/FB approach, on the contrary, can be reduced by the PI-dominant feedback loop, which in turn, improved the compensation by using the CIII-FF/FB method.

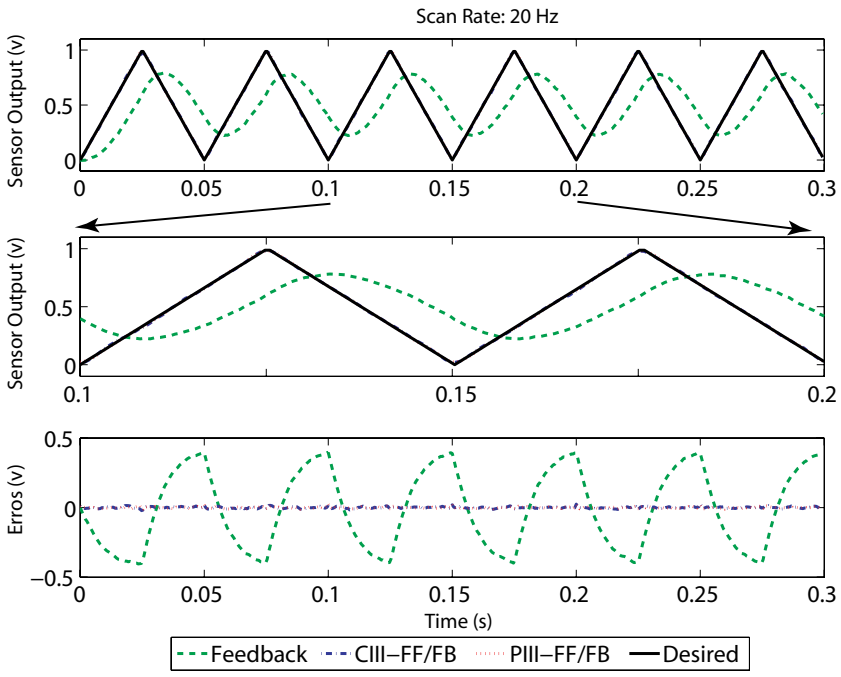

Figure 3.7: The comparison of the force tracking by using the PI-notch-filter feedback only, with that by using the CIII-FF/FB control, and that by the PIII-FF/FB control for the scan rate of 20 Hz.

3.6 Summary

Two architectures of inversion-based iterative feedforward-feedback control have been compared. The experiment result shows that the implementation of II-FF/FB can effectively compensate the hysteresis and vibrational dynamics effects compared to feedback control. Specially, precision position control can be achieved in the high-speed positioning using PIII-FF/FB approach compared to CIII-FF/FB approach. The position error can maintain at 7.95% even at 120 Hz.

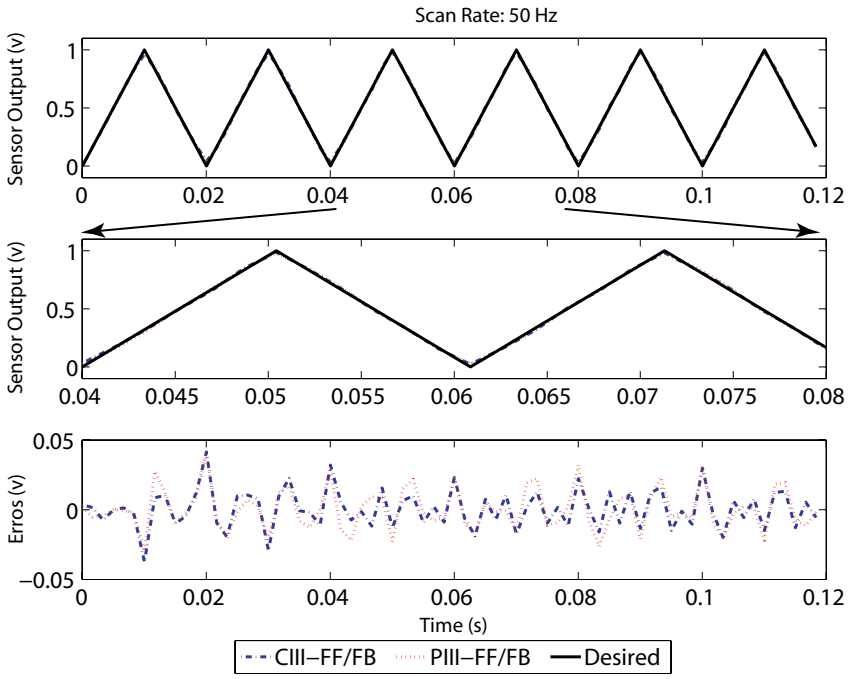

Figure 3.8: The comparison of the force tracking by using the PI-notch-filter feedback only, with that by using the CIII-FF/FB control, and that by the PIII-FF/FB control for the scan rate of 50 Hz.

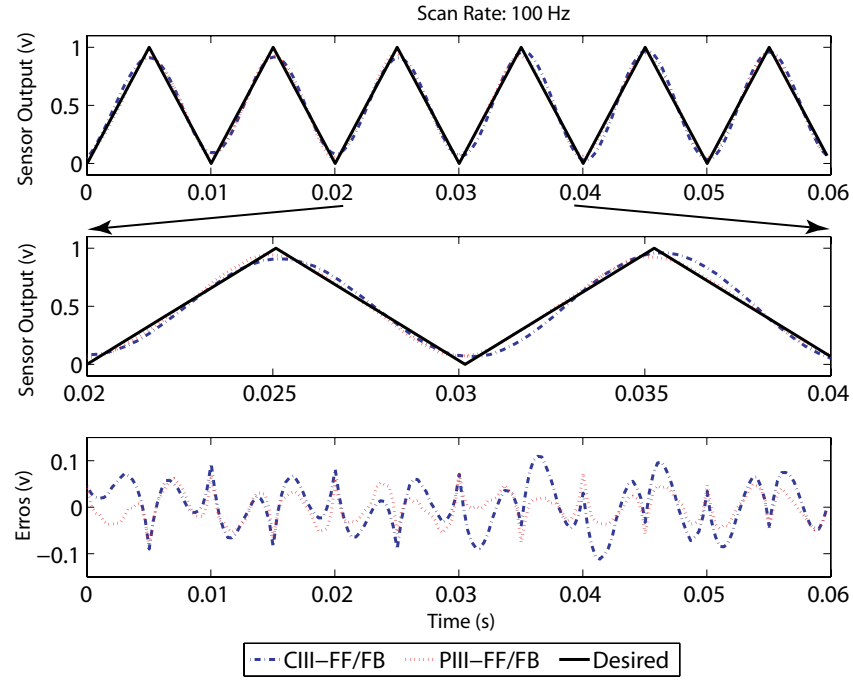

Figure 3.9: The comparison of the force tracking by using the PI-notch-filter feedback only, with that by using the CIII-FF/FB control, and that by the PIII-FF/FB control for the scan rate of 100 Hz.

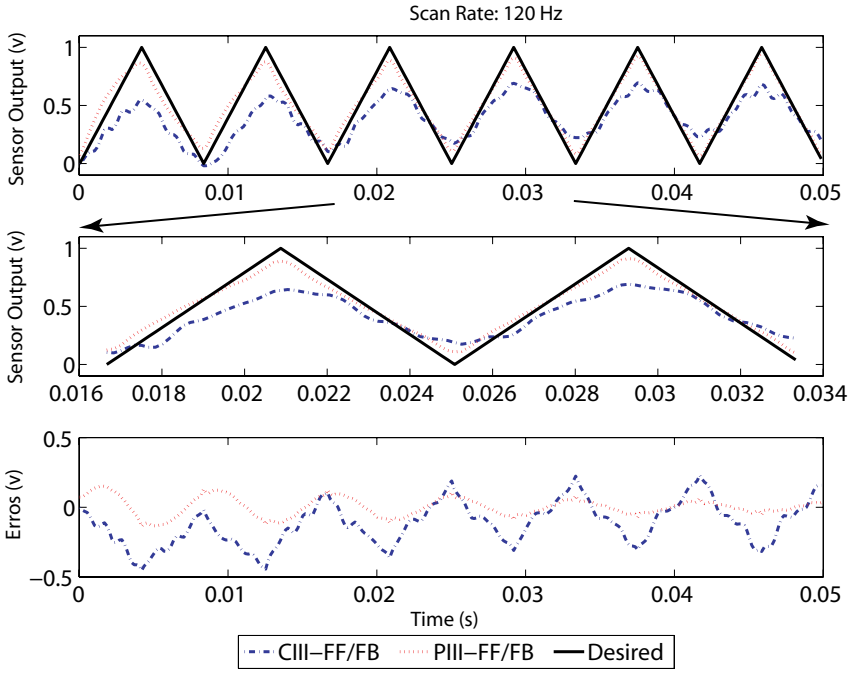

Figure 3.10: The comparison of the force tracking by using the PI-notch-filter feedback only, with that by using the CIII-FF/FB control, and that by the PIII-FF/FB control for the scan rate of 120 Hz.

Table 3.2: Comparison of the tracking errors ($E_M(\%)$ and $E_{RMS}(\%)$) by using the PI controller, CIII-FF/FB and PIII-FF/FB approach at different scan rates.

	$E_M(\%)$			$E_{RMS}(\%)$		
Scan Rate (Hz)	PI	CIII	PIII	PI	CIII	PIII
1	17.54	6.25	5.80	12.14	2.35	2.32
10	29.74	5.67	5.77	15.99	2.42	2.95
30	49.1	6.88	6.14	28.3	3.06	3.28
60		10.64	7.74		4.23	4.68
120		8.11	11.5		4.03	8.75

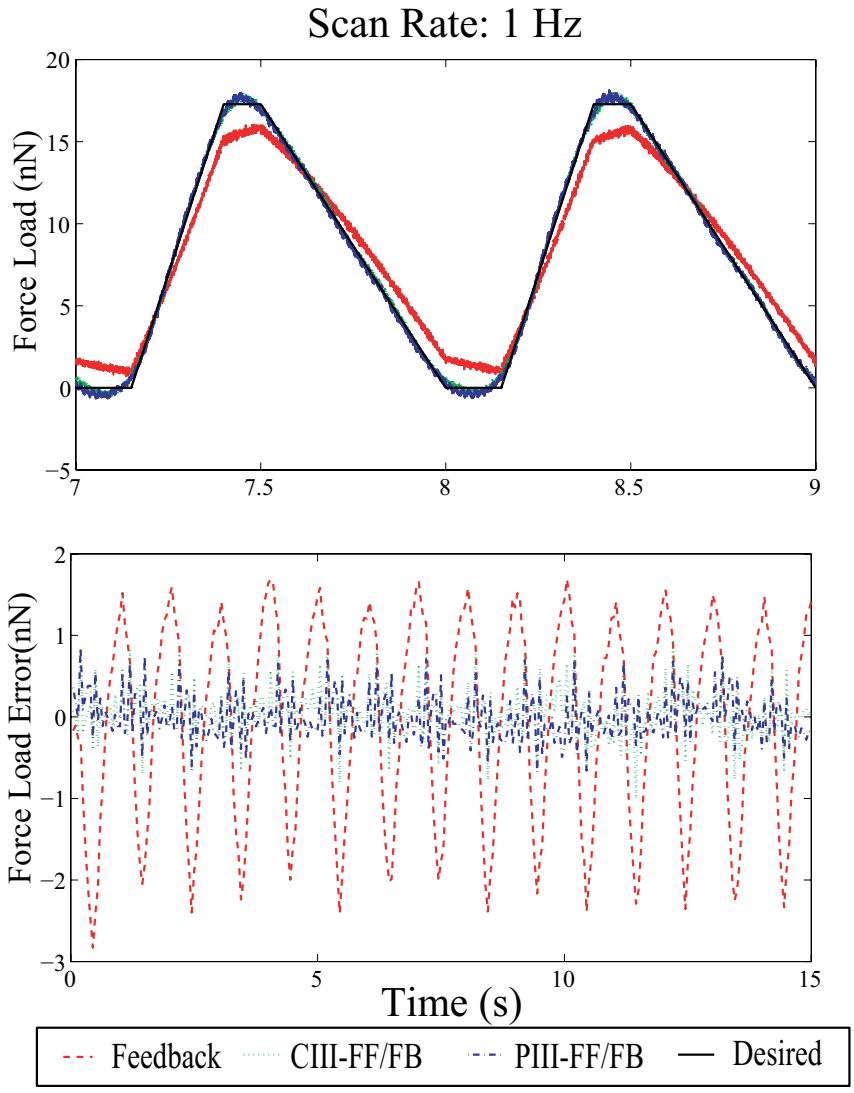

Figure 3.11: The comparison of the force tracking by using the PI-notch-filter feedback only, with that by using the CIII-FF/FB control, and that by the PIII-FF/FB control for the force load rate of 1 Hz.

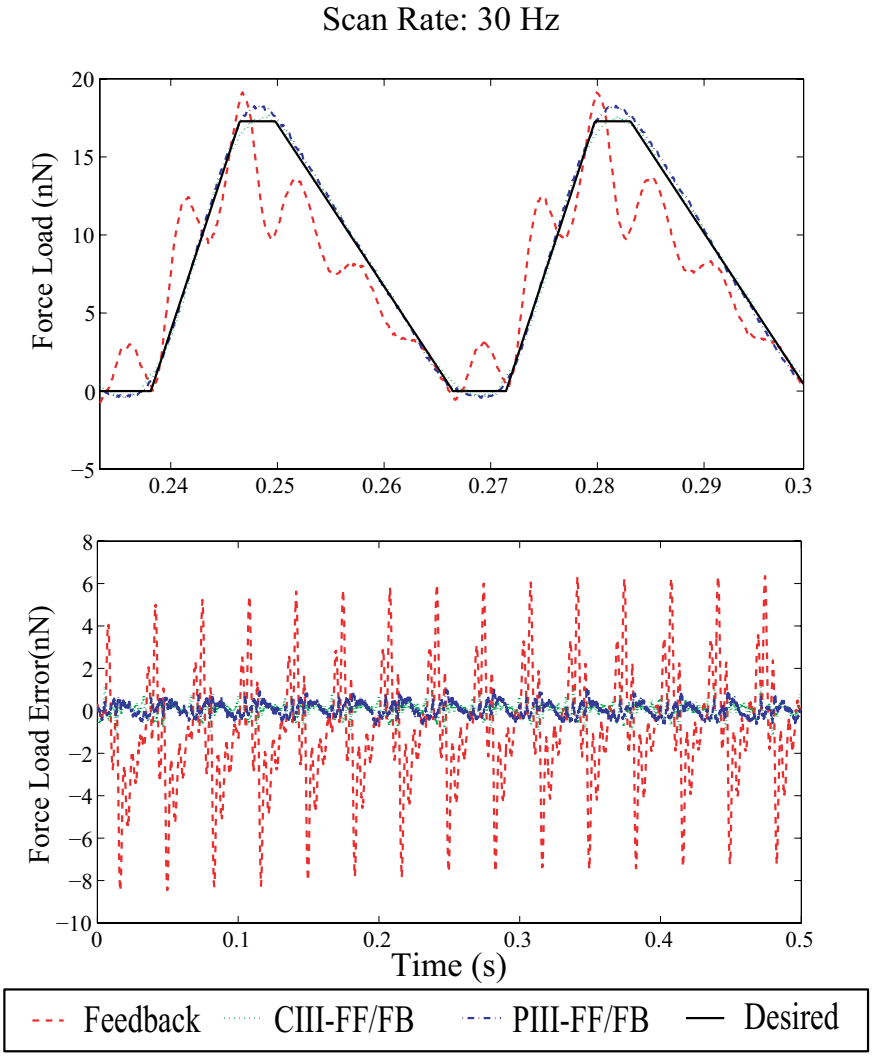

Figure 3.12: The comparison of the force tracking by using the PI-notch-filter feedback only, with that by using the CIII-FF/FB control, and that by the PIII-FF/FB control for the force load rate of 30 Hz.

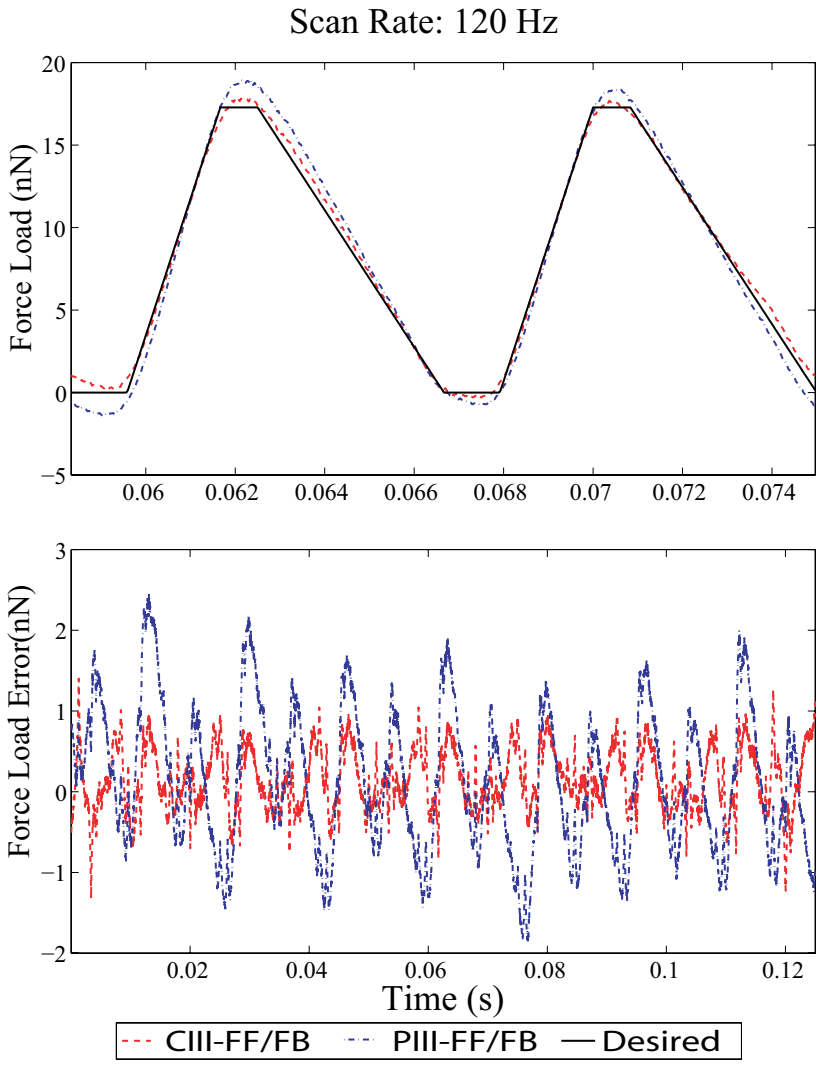

Figure 3.13: The comparison of the force tracking by using the CIII-FF/FB control, and that by the PIII-FF/FB control for the force load rate of 120 Hz.

Chapter 4

Conclusion

We presented the development of inversion-based iterative feedforward-feedback (II-FF/FB) approach in this thesis. Its applications include the high-speed force load in nanomechanical property measurement of soft materials in liquid and high-speed nanopositioning control with piezoelectric actuators. High-speed nanopositioning is widely applied in various areas. However, the precision tracking of the desired trajectory are challenged by various adverse effects. The typical adverse effects in the nanomechanical measurement in liquid includes thermal drift effect, the reduction of the signal to noise ratio, and the hysteresis and the vibrational dynamics effects of the piezoelectric actuators (used to position the probe relative to the sample), particularly during high-speed measurements.

This research focused on the development two II-FF/FB approaches to tackle these challenges in practical applications. First, the II-FF/FB was developed by inverting the closed-loop system dynamics, and then updating and correcting the inversion-based input through iterations (called the closed-loop injection II-FF/FB, CIII-FF/FB technique). A feedback controller with a notch filter was utilized to improve the robustness of the entire system against dynamics uncertainties and the gain margin of the closed-loop system. The proposed CIII-FF/FB technique was implemented in experiments to the nanomechanical property measurement of a poly (dimethylsiloxane) (PDMS) sample in liquid. The experimental results showed that by using the CIII-FF/FB technique, precision tracking of the desired force load profile could be achieved in high speed nanomechanical measurement of soft materials in liquid.

In addition, we also studied the alternative approach to the II-FF/FB approach by

inverting the plant dynamics to generate the feedforward input, and injecting the feedforward input into the feedback loop by augmenting it to the feedback one (called the plant-injection II-FF/FB, PIII-FF/FB technique). These two II-FF/FB techniques, the CIII-FF/FB and PIII-FF/FB techniques were comparatively studied in the nanopositioning tracking of a piezo-bimorph actuator and the force-load profile tracking in nanomechanical measurements in liquid. The experimental results were analyzed and discussed to compare the performance of these two approaches under various conditions.

In the future, there is much more work to be done. First, the convergence analysis of PIII-FF/FB approach should be further discussed so that the algorithm will converge to the desired input which leads to the exact tracking of the desired trajectory. Then two approaches will be implemented to quantitatively study the nanomechanical measurement, such as the rate-dependent elastic modulus of the biological cells.

Appendix A

Matlab Code

```
%%%%%%%%%%%%%%%%%%%%%%%%%%%%%%%%%%%%%%%%%%%%%%%%%%%%%%%%%%%%%%%%%%%%%%%%%%%%%%%%
% File Name: main.m
% Function: inversion-based iterative control main file
%%%%%%%%%%%%%%%%%%%%%%%%%%%%%%%%%%%%%%%%%%%%%%%%%%%%%%%%%%%%%%%%%%%%%%%%%%%%%%%%
clc;format short ;close all; clear all
%%%%%%%%%%%%%%%%%%%%%%%%%%%%%%%%%%%%%%%%%%%%%%%%%%%%%%%%%%%%%%%%%%%%%%%%%%%%%%%%
% 1. Parameters needed for User  to define
%%%%%%%%%%%%%%%%%%%%%%%%%%%%%%%%%%%%%%%%%%%%%%%%%%%%%%%%%%%%%%%%%%%%%%%%%%%%%%%%
%   Parameter needed to change%%%%%%%%%%%%%%%%%%%%%%%%%%%%%%%%%%%%%%%%%%%%%%%%%%%
%%%%%%%%%
first_input_scale= 1;  % Scaling factor for first input data from desired
 %trajectory
trj_type=2  ;       % Desired trajectory type 1 for triangle, 2 for random
sim_on=0    ;           %        1 for simulation
                        %        0 for experimental measurement
num_iter=6  ;           % Number of Iteration
%%%%%%%%%%%%%%%%%%%%%%%%%%%%%%%%%%%%%%%%%%%%%%%%%%%%%%%%%%%%%%%%%%%%%%%%%%%%%%%%
if trj_type==1          %   type 1 for triangle
    Amp=2;                 % Desired Amplitude size
    Hz_desired=10;             % Experiment Speed (Frequency in Hz)
    periods=19;    % Number of Periodes to reach steady states
    ave_prd=floor(periods*0.5)  ;      % number of periods to take average
    Actual_smpl_rate=30;    % Data Acquisition system sampling rate in KHz
```

```
    cut_off_frq=Hz_desired*20;
    eff_frq_rto=(cut_off_frq*10)/Actual_smpl_rate/1000*2;
    triangle_coeff=0.5;
    offset_1=0.5;
else
    Hz_desired=120;
    Actual_smpl_rate=30;
    Amp=1;
    offset=0;
    cut_off_frq=300;
    eff_frq_rto=(cut_off_frq*1)/Actual_smpl_rate/1000*2;
    triangle_coeff=0.5;
    ini_point=0;
end
xpcv.mode='TCPIP';      % Mode selection to transfer data into external PC
xpcv.IP='192.168.0.1'; % IP selection to transfer data into external PC
xpcv.port='22222';      % port number selection to transfer
%data into external PC
scale=10^4;   %   system pole and zero scale factor (only for simulation)
%%%%%%%%%%%%%%%%%%%%%%%%%%%%%%%%%%%%%%%%%%%%%%%%%%%%%%%%%%%%%%%%%%%%%%%%%%%%
% 1-1. Desired trajectory generation (triangle example)
% y_desired: desired trajectory data
% t_desired: desired time data related with 'y_desired'
%%%%%%%%%%%%%%%%%%%%%%%%%%%%%%%%%%%%%%%%%%%%%%%%%%%%%%%%%%%%%%%%%%%%%%%%%%%%
if trj_type==1
    [y_desired, t_desired]=triangle_gen(Actual_smpl_rate,Hz_desired,Amp);
else
    [y_desired, t_desired]=PDMS_ramp(Actual_smpl_rate,Hz_desired,offset,
    ini_point,triangle_coeff);%%%%desired signal
```

```
end
    save desired_trajectory y_desired t_desired

load desired_trajectory

if sim_on==1
    %%%%%%%%%%%%%%%%%%%%%%%%%%%%%%%%%%%%%%%%%%%%%%%%%%%%%%%%%%%%%%%%%%%%%%%%%%%%
    % 1- 2. Basic System setup only for simulation
    %%%%%%%%%%%%%%%%%%%%%%%%%%%%%%%%%%%%%%%%%%%%%%%%%%%%%%%%%%%%%%%%%%%%%%%%%%%%

    % System setup
    load sys  %retruns cn,cdn for transfer function from
                    %file z_dir_fre_resp_3001
              % Used system with 6 poles and 4 zeros

    %system scaling process
    n_cn=length(cn);
    for ii=1:n_cn
        cn(ii)=cn(ii)/scale^(ii-1);
    end
    n_cdn=length(cdn);
    for ii=1:n_cdn
        cdn(ii)=cdn(ii)/scale^(ii-1);
    end
    r=n_cdn-n_cn;   %Ralitive degree for AFM
    [A_afm,B_afm,C_afm,D_afm]=tf2ss(cn/scale^r,cdn);
    sys_afm=ss(A_afm,B_afm,C_afm,D_afm);
end
%%%%%%%%%%%%%%%%%%%%%%%%%%%%%%%%%%%%%%%%%%%%%%%%%%%%%%%%%%%%%%%%%%%%%%%%%%%%
% 2. Trial execution by desired trajectory scaled by first_input_scale
```

```
%%%%%%%%%%%%%%%%%%%%%%%%%%%%%%%%%%%%%%%%%%%%%%%%%%%%%%%%%%%%%%%%%%%%%%%%%%%%
    input=(y_desired)'*first_input_scale;  % First trial input scaled
     %down by first_input_scale
    input_initial=input;
%    output=Execution(input,t_desired,periods,xpcv,Actual_smpl_rate,
output_1_prd); % Execution by trial input
    if sim_on==1
        [output,output_combine]=Execution_option1(input,t_desired,xpcv,
 Actual_smpl_rate,sim_on,sys_afm,scale,y_desired,eff_frq_rto,Hz_desired);
 % Execution by trial input
    else
        [output,output_combine]=Execution_option1(input,t_desired,xpcv,
        Actual_smpl_rate,sim_on,[],scale,y_desired,eff_frq_rto,Hz_desired);
        % Execution by trial input
    end
if trj_type==1
        name=char([double(num2str(floor(Hz_desired))) double('Hz_Tri_ave')
        double(num2str(Amp)) double('V_0th')])

        h=figure(8);
        saveas(h,name,'fig')

[Norm_2_pure(1,1),Norm_inf_pure(1,1),Norm_2_pure_per(1,1),
Norm_inf_pure_per(1,1)]=result_compare(output,y_desired,Actual_smpl_rate,
Hz_desired) % Error Norm computation
name=char([double(num2str(floor(Hz_desired))) double('Hz_Tri_pure')
        double(num2str(Amp)) double('V_0th')])
 save(name, 'y_desired','t_desired','input','y_triangle','Hz_desired',
 'output','Actual_smpl_rate','y_trapezoid','Norm_2_pure','Norm_inf_pure',
        'Norm_2','Norm_inf','output_combine')
```

```
        h=figure(8);
        saveas(h,name,'fig')
else
 name=char([double(num2str(floor(Hz_desired))) double('Hz_PDMS_sample_ave')
     double(num2str(Amp)) double('V_0th')])
[Norm_2_pure(1,1),Norm_inf_pure(1,1),Norm_2_pure_per(1,1),
Norm_inf_pure_per(1,1)]=result_compare(output,y_desired,Actual_smpl_rate,
Hz_desired) % Error Norm computation
       name=char([double(num2str(floor(Hz_desired))) double('Hz_PDMS_pure')
       double(num2str(Amp)) double('V_0th')])
save(name, 'y_desired','t_desired','input','Hz_desired','output',
'Actual_smpl_rate','Norm_2_pure','Norm_inf_pure','Norm_2_pure_per',
'Norm_inf_pure_per','output_combine')
        h=figure(8);subplot(211);
        saveas(h,name,'fig')
end
%%%%%%%%%%%%%%%%%%%%%%%%%%%%%%%%%%%%%%%%%%%%%%%%%%%%%%%%%%%%%%%%%%%%%%%%%%%%
% Iterative execution
%%%%%%%%%%%%%%%%%%%%%%%%%%%%%%%%%%%%%%%%%%%%%%%%%%%%%%%%%%%%%%%%%%%%%%%%%%%%
    for iii=1:num_iter
        input=Input_Compute_MIIC(y_desired,input,output,1,eff_frq_rto,
        t_desired(2),Hz_desired,Actual_smpl_rate,input_initial);
        %New input computed by iterative control method
        h=figure(3);subplot(211);xlim([0 cut_off_frq*1000]);subplot(212);
        xlim([0 cut_off_frq*1000]);saveas(h,'system_computed','fig')
        if sim_on==1
        [output,output_combine]=Execution_option1(input,t_desired,xpcv,
        Actual_smpl_rate,sim_on,sys_afm,scale,y_desired,eff_frq_rto,
        Hz_desired); % Execution by trial input
        else
```

```
        [output,output_combine]=Execution_option1(input,t_desired,xpcv,
        Actual_smpl_rate,sim_on,[],scale,y_desired,eff_frq_rto,Hz_desired);
        % Execution by trial input
        end
     [Norm_2_pure(1,iii+1),Norm_inf_pure(1,iii+1),Norm_2_pure_per(1,iii+1),
     Norm_inf_pure_per(1,iii+1)]=result_compare(output,y_desired,
     Actual_smpl_rate,Hz_desired) % Error Norm computation
        if trj_type==1
    name=char([double(num2str(floor(Hz_desired))) double('Hz_Tri_ave')
 double(num2str(Amp)) double('V_') double(num2str(iii)) double('th')])
        else
name=char([double(num2str(floor(Hz_desired))) double('Hz_PDMS_sample_ave')
double(num2str(Amp)) double('V_') double(num2str(iii)) double('th')])
        end
save(name, 'y_desired','t_desired','input','Hz_desired','output',
'Actual_smpl_rate','Norm_2_pure','Norm_inf_pure','Norm_2_pure_per',
'Norm_inf_pure_per','output_combine')
        h=figure(8);
        saveas(h,name,'fig')
    end


%%%%%%%%%%%%%%%%%%%%%%%%%%%%%%%%%%%%%%%%%%%%%%%%%%%%%%%%%%%%%%%%%%%%%%%%
% File Name: PDMS_ramp.m
% Function: Inversion-based iterative control sub-file
%   "Generates desired trajectory and related time data for PDMS
%force load profile"
%%%%%%%%%%%%%%%%%%%%%%%%%%%%%%%%%%%%%%%%%%%%%%%%%%%%%%%%%%%%%%%%%%%%%%%%
function [y_desired, t_desired]=PDMS_ramp(Actual_smpl_rate,Hz_desired,
offset,ini_point,triangle_coeff)
```

```
Ramp1.Ts = 1/Actual_smpl_rate/1000;
Ramp1.tend = 2;
Ramp1.T_Vec = 0:Ramp1.Ts:Ramp1.tend-Ramp1.Ts;
yd_ramp1 = linspace(ini_point, ini_point+offset, length(Ramp1.T_Vec));
Horizon1.Ts = 1/Actual_smpl_rate/1000;
Horizon1.tend = 2 + Ramp1.tend;
Horizon1.T_Vec = Ramp1.tend:Horizon1.Ts:Horizon1.tend-Horizon1.Ts;
yd_horizon1 = linspace(ini_point+offset, ini_point+offset,
length(Horizon1.T_Vec));
SimuCon.Ts = 1/Actual_smpl_rate/1000;
SimuCon.tend = 1/Hz_desired + Horizon1.tend;
SimuCon.T_Vec = Horizon1.tend:SimuCon.Ts:SimuCon.tend-SimuCon.Ts;
yd_triangle = offset+triangle_coeff+triangle_coeff*sawtooth(SimuCon.T_Vec*
2*pi*Hz_desired, 0.5);
y1 = yd_triangle;
for k = 1:14;
    yd_triangle = [yd_triangle y1];
end;
Horizon2.Ts = 1/Actual_smpl_rate/1000;
Horizon2.tend = 2 + SimuCon.tend;
Horizon2.T_Vec = SimuCon.tend:Horizon2.Ts:Horizon2.tend-Horizon2.Ts;
yd_horizon2 = linspace(ini_point+offset, ini_point+offset,
length(Horizon2.T_Vec));
Ramp2.Ts = 1/Actual_smpl_rate/1000;
Ramp2.tend = 2 + Horizon2.tend;
Ramp2.T_Vec = Horizon2.tend:Ramp2.Ts:Ramp2.tend-Ramp2.Ts;
yd_ramp2 = linspace(ini_point+offset, ini_point, length(Ramp2.T_Vec));
T_Vec = (0:2*length(yd_ramp1) + 2*length(yd_horizon1) +
length(yd_triangle) - 1).*SimuCon.Ts;
yd = [yd_ramp1 yd_horizon1 yd_triangle yd_horizon2 yd_ramp2];
```

```
y_desired=yd;
t_desired=T_Vec;
figure(1);
plot(t_desired, y_desired);
xlim([0 length(t_desired)/Actual_smpl_rate/1000]);

%%%%%%%%%%%%%%%%%%%%%%%%%%%%%%%%%%%%%%%%%%%%%%%%%%%%%%%%%%%%%%%%%%%%%%%%%%%%
% File Name: Execution_option1.m
% Function: Inversion-based iterative control sub-file
%   "Execute input data with given system and collect output data"
%%%%%%%%%%%%%%%%%%%%%%%%%%%%%%%%%%%%%%%%%%%%%%%%%%%%%%%%%%%%%%%%%%%%%%%%%%%%
function [output,output_2]=Execution_option1(input,t_desired,xpcv,
Actual_smpl_rate,sim_on,sys_afm,scale,y_trapezoid,eff_frq_rto,Hz_desired)
%%%%%%%%%%%%%%%%%%%%%%%%%%%%%%%%%%%%%%%%%%%%%%%%%%%%%%%%%%%%%%%%%%%%%%%%%%%%
% 1. Input data computation
%%%%%%%%%%%%%%%%%%%%%%%%%%%%%%%%%%%%%%%%%%%%%%%%%%%%%%%%%%%%%%%%%%%%%%%%%%%%
    len_input=length(input);    % size of input
    len_desired=length(y_trapezoid);
    Data=input;
    Data1=y_trapezoid;
%%%%%%%%%%%%%%%%%%%%%%%%%%%%%%%%%%%%%%%%%%%%%%%%%%%%%%%%%%%%%%%%%%%%%%%%%%%%
% 3. Execution into system with new input computed from inversion
%%%%%%%%%%%%%%%%%%%%%%%%%%%%%%%%%%%%%%%%%%%%%%%%%%%%%%%%%%%%%%%%%%%%%%%%%%%%
        %   Input data sending block into xPC  %%%%%%%%%%%%%%%%%%%%%%%%%%%%%
   if sim_on==0
     xpcbytes2file('white_x.dat',Data); %write data to a file in host-pc %
        H_ftp=xpctarget.ftp(xpcv.mode,xpcv.IP,xpcv.port);
        % Create xPC Target FTP object
        H_fsys=xpctarget.fs(xpcv.mode,xpcv.IP,xpcv.port);
        % Create xPC Target file system object
```

```
H_fsys.removefile('white_x.dat');% Remove a file from target pc %
H_ftp.put('white_x.dat');% Transfer a file from host to target%
    tg=xpctarget.xpc;
    tg.load('model_3');
tg.SampleTime=1/Actual_smpl_rate/1000;% Setting up sampling speed
try
%   Executing input signal block %%%%%%%%%%%%%%%%%%%%%%%%%%%%%%%%
tg.StopTime=(len_desired)/Actual_smpl_rate/1000;
% Setting up system execution time
tg.start                                                          %
%%%%%%%%%%%%%%%%%%%%%%%%%%%%%%%%%%%%%%%%%%%%%%%%%%%%%%%%%%%%%%%%%%%
catch
end
Out_log = getlog(tg, 'OutputLog');
% Collecting all the output data
time_outlog=Out_log(:,4);   % Time data collected
output_1=Out_log(1:length(input),1);
output_2=Out_log(1:length(input),2);
output_3=Out_log(1:length(input),3);
output=output_1;
len_o=length(output_1);
figure(7);plot((0:len_o-1)/Actual_smpl_rate/1000,output);grid on
title('System output');
else        % Simulation case
Data_time=(0:length(Data)-1)'*(t_desired(2)-t_desired(1))*scale;
[output_1,time_outlog] =lsim(sys_afm,Data,Data_time);
len_o=length(output_1);
Noise=randn(size(output_1))*.002+0.182;
output_1=output_1+Noise;
output_raw=output_1;
```

```
        output_filtfilt=output_1;
        output_2=output_1;
        figure(7);plot((0:len_o-1)/Actual_smpl_rate/1000,output_raw);
        grid on
        title('System output')
    end

%%%%%%%%%%%%%%%%%%%%%%%%%%%%%%%%%%%%%%%%%%%%%%%%%%%%%%%%%%%%%%%%%%%%%%%%%%%%
% File Name: result_compare.m
% Function: Inversion-based iterative control sub-file
%   "Error Norm computation"
%%%%%%%%%%%%%%%%%%%%%%%%%%%%%%%%%%%%%%%%%%%%%%%%%%%%%%%%%%%%%%%%%%%%%%%%%%%%

function [Norm_2,Norm_inf,Norm_2_per,Norm_inf_per]=result_compare(output,
y_desired,Actual_smpl_rate,Hz_desired)
    yd_triangle=y_desired(4*Actual_smpl_rate*1000+1:length(y_desired)-
    4*Actual_smpl_rate*1000);
    y_desired=yd_triangle';
    output=output(4*Actual_smpl_rate*1000+1:length(output)-
    4*Actual_smpl_rate*1000);
    len_output=length(output);
    Y_D_2=[y_desired];
    Diff=(output-y_desired);% Error data
    figure(8);
    subplot(211);plot((0:len_output-1)/Actual_smpl_rate/1000,output,
    (0:len_output-1)/Actual_smpl_rate/1000,y_desired,'r--');
    legend('output','desired');
    subplot(212),plot((0:len_output-1)/Actual_smpl_rate/1000,Diff);
    title('Tracking Error');
    Norm_2=norm(Diff,2)/sqrt(length(Diff))*100;%/norm(y_desired,2)*100;
```

```
    % 2 Norm of error in percentage
    Norm_inf=norm(Diff,inf)*100;%/(max(y_desired)-min(y_desired))*100;
    % inf Norm of error in percentage
    Norm_2_per=norm(Diff,2)/norm(Y_D_2,2)*100;%/norm(y_desired,2)*100;
    % 2 Norm of error in percentage
    Norm_inf_per=norm(Diff,inf)/norm(Y_D_2,inf)*100;%/(max(y_desired)-
    min(y_desired))*100; % inf Norm of error in percentage

%%%%%%%%%%%%%%%%%%%%%%%%%%%%%%%%%%%%%%%%%%%%%%%%%%%%%%%%%%%%%%%%%%%%%%%%%%%%
% File Name: Input_Compute.m
% Function: Modeless Inversion-based iterative control sub-file
%   " Generates new control inputs by Inversion-based iterative control
%   method"
%%%%%%%%%%%%%%%%%%%%%%%%%%%%%%%%%%%%%%%%%%%%%%%%%%%%%%%%%%%%%%%%%%%%%%%%%%%%
function input=Input_Compute_MIIC(y_d,input,output,periods,eff_frq_rto,dt,
Hz_desired,Actual_smpl_rate,input_initial)
y_desired_new=y_d';
len_input=length(input);
%%%%%%%%%%%%%%%%%%%%%%%%%%%%%%%%%%%%%%%%%%%%%%%%%%%%%%%%%%%%%%%%%%%%%%%%%%%%
% 1. Duplicate input, output and desired trajectory
%%%%%%%%%%%%%%%%%%%%%%%%%%%%%%%%%%%%%%%%%%%%%%%%%%%%%%%%%%%%%%%%%%%%%%%%%%%%
input_1=input(1:len_input);
output_1=output(1:len_input);
y_desired_1=y_desired_new(1:len_input);

for ii=2:periods
    input=[input;input_1];
    output=[output;output_1];
    y_desired_new=[y_desired_new;y_desired_1];
end
```

```
if periods==1
    input=input_1;
    output=output_1;
    y_desired_new=y_desired_1;
end
    ave_input=0;
    ave_output=0;
    ave_y_desired_new=0;
    input=input-ave_input;
    output=output-ave_output;
    y_desired_new=y_desired_new-ave_y_desired_new;
%%%%%%%%%%%%%%%%%%%%%%%%%%%%%%%%%%%%%%%%%%%%%%%%%%%%%%%%%%%%%%%%
% 2. Discrete Fast Fourier Transform
%%%%%%%%%%%%%%%%%%%%%%%%%%%%%%%%%%%%%%%%%%%%%%%%%%%%%%%%%%%%%%%%
U = fft(input);
Y=fft(output);
Y_d = fft(y_desired_new);
G=    Y./U;
len_f=floor(length(U)/2)+1;% Number of Frequcncy component of input,
output, desired tracking output after FFT transform
%%%%%%%%%%%%%%%%%%%%%%%%%%%%%%%%%%%%%%%%%%%%%%%%%%%%%%%%%%%%%%%%
% 3. Find new input
%%%%%%%%%%%%%%%%%%%%%%%%%%%%%%%%%%%%%%%%%%%%%%%%%%%%%%%%%%%%%%%%
len_H=floor(len_f*eff_frq_rto);    % Size of data to be used in inversion.
%Specific value (eff_frq_rto < 1) can be adjusted by user.
% Finding proper even or odd number for len_H depending on input data size
if length(U)/2==floor(length(U)/2)
    if len_H/2==floor(len_H/2)
        len_H=len_H-1;
        disp('Case 1')
```

```
    else
        disp('Case 2')
    end
else
    if len_H/2==floor(len_H/2)
        disp('Case 3')
    else
        disp('Case 4')
        len_H=len_H-1;
    end
end
%%%%%%%%%%%%%%%%%%%%%%%%%%%%%%%%%%%%%%%%%%%%%%%%%%%%%%%%%%%%%%%%%%%%%%%
% Core input computation
% U_k+1(jw)=U_k(jw) / Y_k(jw) * Y_d(jw)
%%%%%%%%%%%%%%%%%%%%%%%%%%%%%%%%%%%%%%%%%%%%%%%%%%%%%%%%%%%%%%%%%%%%%%%
    sm_out_idx=find(abs(Y(1:len_f))<10^-8);
    G_pre=Y(1:len_f)./U(1:len_f);
lnth=len_input;
fD=1/dt*(0:floor(lnth/2))/lnth;
    new_u_half_pre=1./G_pre.*Y_d(1:len_f);
    % First Half size data from inversion
    new_u_half_pre(sm_out_idx)=zeros(size(sm_out_idx));
    % Ignore small output frequency component

    new_u_half_pre(len_H+1:len_f,1)=zeros(len_f-len_H,1);
    % First Half size data from inversion

    x=2:10;
    y=abs(G_pre(2:10));
    new_u_half_pre(1)=new_u_half_pre(1)-length(Y)*((ave_y_desired_new-
```

```
    ave_output)/abs(G_pre(2)))+length(Y)*ave_input;
%%%%%%%%%%%%%%%%%%%%%%%%%%%%%%%%%%%%%%%%%%%%%%%%%%%%%%%%%%%%%%%%%%%%%%%
% 4. Input Generation for one period
%%%%%%%%%%%%%%%%%%%%%%%%%%%%%%%%%%%%%%%%%%%%%%%%%%%%%%%%%%%%%%%%%%%%%%%
if length(U)/2==floor(length(U)/2)
    disp('Even')
    new_u_half_post=conj(flipud(new_u_half_pre));% Second half size data
    new_u=[new_u_half_pre ;new_u_half_post(2:len_f-1)];
    % Combining First and second half size data
    new_input=real(ifft(new_u));
    % Generation new multiple periods of input in real value
else
    disp('Odd')
    new_u_half_post=conj(flipud(new_u_half_pre));% Second half size data
    new_u=[new_u_half_pre ;new_u_half_post(1:len_f-1)];
    % Combining First and second half size data
    new_input=real(ifft(new_u));
    % Generation new multiple periods of input in real value
end
    if periods==1
        input=[new_input(length(new_input));new_input];
    else
        input=new_input((len_input-1)*floor(periods/2):(len_input-1)*
        (floor(periods/2)+1)); % Picking one representing input period
    end
    input=input(1:length(input)-1);
    figure(1);plot((0:length(input)-1)/Actual_smpl_rate/1000,input);
    title('Input signal')
```

```
%%%%%%%%%%%%%%%%%%%%%%%%%%%%%%%%%%%%%%%%%%%%%%%%%%%%%%%%%%%%%%%%%%%%%%%%%%%%
% File Name: frequency_response.m
% Function: Compute the frequency response and design the notch filter
%%%%%%%%%%%%%%%%%%%%%%%%%%%%%%%%%%%%%%%%%%%%%%%%%%%%%%%%%%%%%%%%%%%%%%%%%%%%
clc;close all;clear all;
f_sample = 40000; %define sample frequency maximum of f_sample = 100k
d = load('bode_plot_amp3_off0_withoutnotch.mat');
output2 = d.output2((2*f_sample+1):(17*f_sample));
output1 = d.output1((2*f_sample+1):(17*f_sample));
target_time=15;
L=target_time*f_sample;
f = f_sample/2*linspace(0,1,L/2);
Low_limit = 1;
High_limit = 500;
f_max_index = find(f<High_limit);
f_max_index = f_max_index(length(f_max_index))+1;
f_min_index = find(f<Low_limit);
f_min_index = f_min_index(length(f_min_index))+1;
ave_output2 = mean(output2);%(len_z_d*(total_periods-1)+
1:len_z_d*total_periods)
output2 = output2 - ave_output2;
ave_output1 = mean(output1);%(len_z_d*(total_periods-1)+
1:len_z_d*total_periods)
output1 = output1 - ave_output1;
x_fft1=fft(output2,L);
out_fft1 = fft(output1,L);
complex_value = out_fft1(f_min_index:f_max_index)./
x_fft1(f_min_index:f_max_index);
mag1 = abs(complex_value);
phase1 = angle(complex_value)*180/pi;
```

```
Output=(output1);%
Input=(output2);
Ts=1/f_sample;
z1 = iddata(Output,Input,Ts);
zd1 = detrend(z1);
zd_fdr1 = spafdr(zd1,[],{1*2*pi,High_limit*2*pi,500});
zd_fdr1.Frequency = zd_fdr1.Frequency/(2*pi);
H1=freqresp(zd_fdr1);
H = (H1(:));
H_abs = (abs(H1(:)));
H_phase = phase(H1(:))*180/pi;
[b,a]=invfreqs(H,zd_fdr1.Frequency*2*pi,5,7);
sys = tf(b,a);
mag_value=out_fft1(f_min_index:L/2)./x_fft1(f_min_index:L/2);
w1=zd_fdr1.Frequency*2*pi;
bw=linspace(1,500,7486)*2*pi;
mmm=120;
nnn=70*500/(2.2918^2+mmm^2);
m=nnn*conv([1 -2*pi*(-2.2918+mmm*i)],[1 -2*pi*(-2.2918-mmm*i)]);
n=conv([1 -2*pi*(-70)],[1 -2*pi*(-500)]);
sysnotch=tf(m,n)
syscomposite=sys*sysnotch;
notch_complex=freqs(m,n,bw)';
total_complex=notch_complex.*complex_value;
[magnotch,phasenotch]=bode(sysnotch,bw);
[magcomposite,phasecomposite]=bode(syscomposite,w1);
SZ=length(complex_value);
for ii=1:SZ
    Mag(ii)=mag1(ii); %#ok<AGROW>
    Phase(ii)=phase1(ii); %#ok<AGROW>
```

```
    Magnotch(ii)=abs(notch_complex(ii)); %#ok<AGROW>
    Phasenotch(ii)=angle(notch_complex(ii)); %#ok<AGROW>
    Magcomposite(ii)= abs(total_complex(ii)); %#ok<AGROW>
    Phasecomposite(ii)= angle(total_complex(ii)); %#ok<AGROW>
end
figure(25),subplot(211);
semilogx(bw/2/pi,20*log10(mag1));hold on;
semilogx(bw/2/pi,(20*log10(Magnotch)),'r'); hold on;
semilogx(bw/2/pi,(20*log10(Magcomposite)),'g');
xlim([min(bw/2/pi) max(bw/2/pi)]);
ylabel('Amplitude(dB)');
legend('bimorph','notch filter','composite system','best');
title('plant bode plot');
subplot(212);
semilogx(bw/2/pi,unwrap(phase1));hold on;
semilogx(bw/2/pi,unwrap(Phasenotch*180/pi),'r');hold on;
semilogx(bw/2/pi,unwrap(Phasecomposite*180/pi),'g');
xlim([min(bw/2/pi) max(bw/2/pi)]);
xlabel('Frequency(Hz)');
ylabel('Phase(degrees)');
legend('bimorph','notch filter','composite system','best');
disp('******to the end*******');

%%%%%%%%%%%%%%%%%%%%%%%%%%%%%%%%%%%%%%%%%%%%%%%%%%%%%%%%%%%%%%%%%%%%%%%%%%%%
% File Name: plot_result.m
% Function: plot the experiment results
%%%%%%%%%%%%%%%%%%%%%%%%%%%%%%%%%%%%%%%%%%%%%%%%%%%%%%%%%%%%%%%%%%%%%%%%%%%%
Actual_smpl_rate=30;
down=1;
dn=500;
```

```
fb_2=load('1Hz_PDMS_pure1V_0th');
opt1=load('1Hz_PDMS_sample_ave1V_2th');
opt2=load('1Hz_PDMS_sample_ave1V_2th_option2');
freq_desired=fb_2.Hz_desired;
output_2=fb_2.output;
o_periods=output_2(4*Actual_smpl_rate*1000+7/freq_desired*
Actual_smpl_rate*1000+1:length(output_2)-4*Actual_smpl_rate*
1000-6/freq_desired*Actual_smpl_rate*1000);
output_2=output_2(4*Actual_smpl_rate*1000+1:length(output_2)-
4*Actual_smpl_rate*1000);
output_2=output_2(1:down:length(output_2));
desired=fb_2.y_desired';
d_periods=desired(4*Actual_smpl_rate*1000+7/freq_desired*Actual_smpl_rate*
1000+1:length(desired)-4*Actual_smpl_rate*1000-6/freq_desired*
Actual_smpl_rate*1000);
desired=desired(4*Actual_smpl_rate*1000+1:length(desired)-
4*Actual_smpl_rate*1000);
desired=desired(1:down:length(desired));
option1=opt1.output;
o1_periods=option1(4*Actual_smpl_rate*1000+7/freq_desired*Actual_smpl_rate*
1000+1:length(option1)-4*Actual_smpl_rate*1000-6/
freq_desired*Actual_smpl_rate*1000);
option1=option1(4*Actual_smpl_rate*1000+1:length(option1)-
4*Actual_smpl_rate*1000);
option1=option1(1:down:length(option1));
option2=opt2.output;
o2_periods=option2(4*Actual_smpl_rate*1000+7/freq_desired*Actual_smpl_rate*
1000+1:length(option2)-4*Actual_smpl_rate*1000-
6/freq_desired*Actual_smpl_rate*1000);
option2=option2(4*Actual_smpl_rate*1000+1:length(option2)-
```

```
4*Actual_smpl_rate*1000);
option2=option2(1:down:length(option2));
t=(1:length(output_2))/Actual_smpl_rate/1000*down;
t1=(0:length(o_periods)-1)/Actual_smpl_rate/1000+7/freq_desired;
t=t(1:dn: length(t));
t1=(1:dn:length(t1));
t1=linspace(0,2,length(t1));
option1=option1(1:dn:length(option1));
option2=option2(1:dn:length(option2));
output_2=output_2(1:dn:length(output_2));
d_periods=d_periods(1:dn:length(d_periods));
o1_periods=o1_periods(1:dn:length(o1_periods));
o2_periods=o2_periods(1:dn:length(o2_periods));
o_periods=o_periods(1:dn:length(o_periods));
desired=desired(1:dn:length(desired));
subplot(3,1,1);
h1=plot(t,output_2,'--g',t,option1,'-.b',t,option2,':r',t,desired,'k');
set(h1,'LineWidth',3);
title('Scan Rate: 1 Hz');
xlim([0 6]);
ylim([-0.1 1.1]);
ylabel('Sensor Output (v)');
legend('Feedback','CIII-FF/FB','PIII-FF/FB','Desired','Location',
'NorthOutside','Orientation','horizontal');
subplot(3,1,2);
h2=plot(t1+2/freq_desired,o_periods,'--g',t1+2/freq_desired,o1_periods,'-.b',
t1+2/freq_desired,o2_periods,':r',t1+2/freq_desired,d_periods,'k');
set(h2,'LineWidth',3);
ylabel('Sensor Output (v)');
ylim([-0.1 1.1]);
```

```
subplot(3,1,3);
h3=plot(t,output_2-desired,'--g',t,option1-desired,'-.b',
t, option2-desired,':r');
set(h3,'LineWidth',3);
ylabel('Erros (v)');
xlabel('Time (s)');
ylim([-0.05 0.05]);
xlim([0 6]);
```

Appendix B

Simulink Block Diagrams

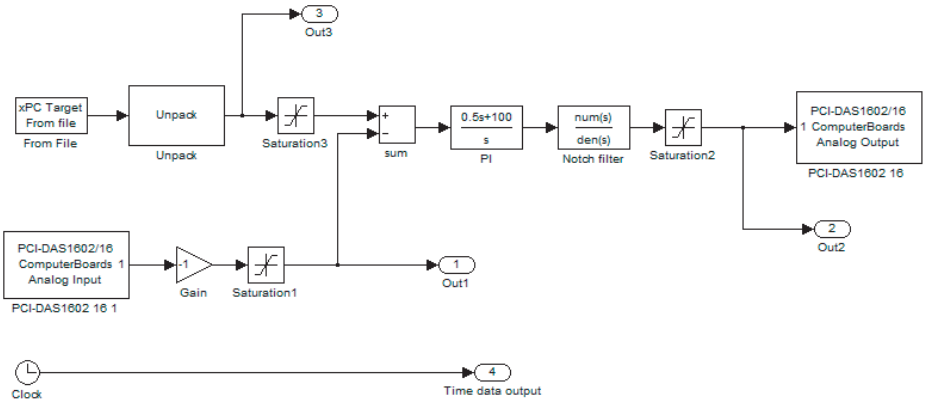

Figure B.1: Simulink block diagram of the experiment.

References

[1] C. J. Wright and I. Armstrong, "The application of atomic force microscopy force measurements to the characterisation of microbial surfaces," *SURFACE AND INTERFACE ANALYSIS*, vol. 38, no. 5, pp. 1419–1428, 2006.

[2] T. Fukuma and S. P. Jarvis, "Biological applications of FM-AFM in liquid environment," in *Noncontact Atomic Force Microscopy* (S. Morita, F. J. Giessibl, and R. Wiesendanger, eds.), NanoScience and Technology, pp. 329–345, Springer Berlin Heidelberg, 2009. 10.1007/978-3-642-01495-6-16.

[3] T. Sulchek, R. Hsieh, J. D. Adams, S. C. Minne, C. F. Quate, and D. M. Adderton, "High-speed atomic force microscopy in liquid," *Review of Scientific Instruments*, vol. 71, no. 5, pp. 2097–2099, 2000.

[4] E. Canetta, A. Duperray, A. Leyrat, and C. Verdier, "Measuring cell viscoelastic properties using a force-spectrometer: influence of protein-cytoplasm interactions," *Biorheology*, vol. 42, no. 5, pp. 321–333, 2005.

[5] A. Fischer-Cripps, "Critical review of analysis and interpretation of nanoindentation test data," *Surface and Coatings Technology*, vol. 200, pp. 4153–4165, April 2006.

[6] A. B. Mann and J. B. Pethica, "Nanoindentation studies in a liquid environment," *Langmuir*, vol. 12, pp. 4583–4586, September 1996.

[7] G. S. Shekhawat, A. Chand, S. Sharma, Verawati, and V. P. Dravid, "High resolution atomic force microscopy imaging of molecular self assembly in liquids using thermal drift corrected cantilevers," *Applied Physics Letters*, vol. 95, pp. 233114–1 to 233114–3, December 2009.

[8] G. M. Clayton, S. Tien, K. K. Leang, Q. Zou, and S. Devasia, "A review of feedforward control approaches in nanopositioning for high-speed spm," *ASME Journal of Dynamic Systems, Measurement and Control*, vol. 131, pp. 061101–1 to 061101–19, 2009.

[9] H.-J. Butt, B. Cappella, and M. Kappl, "Force measurements with the atomic force microscope: Technique, interpretation and applications," *Surface Science Reports*, vol. 59, pp. 1–152, 2005.

[10] M. Plodinec, M. Loparic, and U. Aebi, "Atomic force microscopy for biological imaging and mechanical testing across length scales," *Cold Spring Harb Protocols*, October 2010.

[11] S. ho Moon and M. D. Foster, "Influence of humidity on surface behavior of pressure sensitive adhesives studied using scanning probe microscopy," *Langmuir*, vol. 18, pp. 8108–8115, 2002.

[12] K. Kim, Z. Lin, P. Shriotrya, S. Sundararajan, and Q. Zou, "Iterative control approach to high-speed force-distance curve measurement using AFM: Time dependent response of PDMS," *Ultramicroscopy*, vol. 108, pp. 911–920, 2008.

[13] Y. Wu and Q. Zou, "Iterative control approach to compensate for both the hysteresis and the dynamics effects of piezo actuators," *IEEE Trans. on Control Systems Technology*, vol. 15, pp. 936–944, 2007.

[14] M. Dao, C. Lim, and S. Suresh, "Mechanics of the human red blood cell deformed by optical tweezers," *Journal of the Mechanics and Physics of Solids*, vol. 51, no. 11-12, pp. 2259–2280, 2003.

[15] J. Guck, R. Ananthakrishnan, H. Mahmood, T. Moon, C. Cunningham, and J. K "as, "The optical stretcher: a novel laser tool to micromanipulate cells," *Biophysical Journal*, vol. 81, no. 2, pp. 767–784, 2001.

[16] R. Hochmuth, "Micropipette aspiration of living cells," *Journal of Biomechanics*, vol. 33, no. 1, pp. 15–22, 2000.

[17] C. A. V. Eysden and J. E. Sader, "Frequency response of cantilever beams immersed in viscous fluids with applications to the atomic force microscope: Arbitrary mode order," *Journal of Applied Physics*, vol. 101, pp. 044908–044918, 2007.

[18] Z. Xu, K. Kim, Q. Zou, and P. Shrotriya, "Broadband measurement of rate-dependent viscoelasticity at nanoscale using scanning probe microscope: Poly(dimethylsiloxane) example," *Applied Physics Letters*, vol. 93, pp. 133103–1–133103–3, Sep. 2008.

[19] S. A. S. Asif, K. J. Wahl, and R. J. Colton, "Nanoindentation and contact stiffness measurement using force modulation with a capacitive load-displacement transducer," *Review of Scientific Instruments*, vol. 70, no. 5, pp. 2408–2413, 1999.

[20] E. Canetta, A. Duperray, A. Leyrat, and C. Verdier, "Measuring cell viscoelastic properties using a force-spectrometer: influence of protein-cytoplasm interactions," *Biorheology*, vol. 42, no. 5, pp. 321–333, 2005.

[21] J. A. Butterworth, L. Y. Pao, and D. Y. Abramovitch, "A comparison of control architectures for atomic force microscopes," *Asian Journal of Control*, vol. 11, pp. 175–181, March 2009.

[22] G. M. Clayton, S. Tien, K. Leang, Q. Zou, and S. Devasia, "A review of feedforward control approaches in nanopositioning for high-speed spm," *ASME Journal of Dynamic Systems, Measurement and Control*, vol. 131, pp. 1–19, November 2009.

[23] G. Stein, "Respect the unstable," *IEEE control system magazine*, vol. 23, no. 4, pp. 12–25, 2003.

[24] K.-S. Kim and Q. Zou, "A model-less inversion-based iterative control technique for output tracking: Piezo actuator example," in *Proceedings of American Control Conference*, (Seattle, WA), pp. 2710–2715, June 2008.

[25] Y. Okazaki, "A micro-positioning tool post using a piezoelectric actuator for diamond turning machines,," *Precision Engineering*, vol. 12, no. 3, pp. 151–156, 1990.